# A STUDY OF THE TRANSITION FROM ANNULAR TO DISPERSED REGIME IN TWO-PHASE AIR-WATER FLOW

*by*

JANARDAN TEWARY



DEPARTMENT OF MECHANICAL ENGINEERING

INDIAN INSTITUTE OF TECHNOLOGY, KANPUR

AUGUST, 1972

# A STUDY OF THE TRANSITION FROM ANNULAR TO DISPERSED REGIME IN TWO-PHASE AIR-WATER FLOW

A Thesis Submitted
In Partial Fulfilment of the
Requirements for the Degree of

MASTER OF TECHNOLOGY

by

JANARDAN TEWARY

to the

Department of Mechanical Engineering
Indian Institute of Technology, Kanpur

August, 1972

CERTIFICATE

This is to certify that this work on "A Study of the Transition From Annular to Dispersed Regime in two-phase Air-Water Flow" has been carried out under my supervision and has not been submitted elsewhere for a degree.

G. SRIKANTIAH
Professor and Head
Department of Mechanical Engineering
Indian Institute of Technology
Kanpur (India)

ACKNOWLEDGEMENTS

I am deeply indebted to Dr. G. Srikantiah for his guidance, inspiration and fruitful discussions during the thesis work.

I am grateful to Mr. M.P. Sharma and Mr.M.Prasad for their help, discussion and encouragement during this work.

I would like to thank Mr. P.N. Mishra and Mr. B.S. Arya for their constant help.

I also like to express my thanks to Messrs. R.M. Jha, B.L. Sharma, and my friends Messrs. N.K. Giri, S.K. Chaturvedi, S.K. Gupta and A. Rajamani for their cooperation.

My thanks are also due to Shri Uma Raman Pandey who made a magnificient job of typing.

JANARDAN TEWARY

# CONTENTS

# LIST OF TABLES

# LIST OF FIGURES

# NOMENCLATURE

$A_1$ - Pipe inside Cross sectional area at the upstream pressure tap

$A_2$ - Orifice area at flow temperature

C - Co-efficient of discharge

$C_1$ - Orifice plate thickness

$C_2$ - Leading edge thickness of Orifice plate

$D_1$ - Inside pipe diameter at upstream pressure

$D_2$ - Orifice tap diameter

D - Diameter of test section

f - Friction factor in two-phase flow

$F_r$ - Froud Number

$G_g, G_L$ - Mass velocities of gas and liquid respectively

g - Acceleration due to gravity

$\Delta h$ = Differential pressure across the orifice between pressure taps in upstream and downstream section

$h_w$ - Differential pressure across the orifice

K - Orifice discharge co-efficient

$L, \Delta z$ length of the test-section

M - Molecular weight of the gas

n - Index

$\Delta P$ - Differential pressure in two phase flow

$P_1$ - Absolute static pressure at the upstream pressure tap

$Re$ - Reynold number

$R_m$ - Reynold number of the mixture

$T_1$ - Absolute temperature of the flowing fluid upstream side of the orifice

TPF - Two-phase flow

$U_1$ - Average velocity in the pipe at the upstream pressure tap

$U_2$ - Average velocity through the orifice at flow conditions

$V_*$ - Minimum gas velocity for entrainment

$v_f, v_g$ - Specific volume of liquid and gas respectively

$V_{fg}$ - Specific volume of two phases

$V_m$ - Velocity of the mixture

$\bar{v}$ - Mean specific volume

$V_{gs}, V_{fs}$ - Superficial gas and liquid velocities respectively

$w$ - Flow rate, lbs/hr

$w_g, w_l$ — Flow rate of gas & liquid respectively

$x$ - Air-weight fraction

$X^2$ - Ratio of liquid phase flow pressure drop and gas phase flow pressure drop.

$\alpha$ - An area multiplier which allows for thermal expansion or contraction

$\beta$ - Volumetric Void fraction

$\beta_1$ - Diameter-ratio

$\rho_1, \rho_2$ - Density of air at upstream pressure tap and at downstream pressure tap respectively

$\mu_1$ - Gas law deviation (compressibility) factor

$\sigma$ - Surface-tension

$\mu_g, \mu_f$ - Viscosity of gas and liquid respectively

$\rho_g, \rho_L$ - Density of gas and liquid respectively

$\phi_g^2$ - Ratio of two-phase flow pressure and gas phase flow pressure drop

$\phi_L^2$ - Ratio of two phase flow pressure drop and liquid phase flow pressure drop.

$W_{mix}$ – Flow rate of mixture.

$W_o', W_g'$ – Reduced liquid & gas velocities respectively.

## SYNOPSIS

The regime transition and pressure drop of two-phase air-water co-current upward flow in a vertical circular channel has been investigated experimentally. The transition of dispersed flow to annular flow at low pressures has been studied, visual observation of flow regimes has been made using still photographs.

The test channel is made up of 16 mm O.D. and 11.5 mm I.D. pyrex glass tube. Actual length of the test channel is 1400 mm but the test length was 800 mm only. The range of parameters studied are pressure 1.1736 kgf/cm$^2$ abs.; 1.3142 kgf/cm$^2$ abs. and 1.5954 kgf/cm$^2$ abs.; flow rate of air 11.78 kgm/hr to 40.3 kgm/hr; flow rate of water 0.9 kgm/hr to 1.44 kgm/hr.

Tables and curves representing the transition with pressure as parameter are presented. Also the variation of pressure drop with air-weight fraction is presented. Pressure drop varied from 280 mm of water per meter to 1021 mm of water per meter while air weight fraction variedfrom 91.8% to 97.2%.

The sequence of photographs which includes the transition has been also presented starting from the dispersed flow to annular flow. The experimental data represent an extension of Baker's plot. The result is in

good agreement with the prediction of O.A.Kremnev et al who presented their results in terms of gms. of water per cubic meter of air vs. superficial velocities of air for dispersed flow.

Suggestions for further experimental and theoretical research are presented.

# I INTRODUCTION

## 1.1 General :

The study of two phase flows with either single or multi component fluids has led in recent years to an accumulation of a vast amount of literature[1], because of the importance of two-phase flow in the nuclear, space, chemical and agricultural fields. Fluidised beds for reduction of uranium ore and ground-water flows to wells etc. are the examples of solid-liquid two-phase flow. Rocket exhausts containing ash or unburnt metal powder is the example of solid-gas two-phase flow. Two-phase gas-liquid flows are found to exist in boilers, condensers, refrigerators, natural gas pipe lines, gasoline-engine manifolds and nuclear reactors.

The flow of both gas and liquid in the same direction in a conduit is known as co-current two-phase gas-liquid flow.

Two-phase flows have been studied for several decades, but the earlier investigations were mainly devoted to practical problems of petroleum and chemical engineering. Although a significant amount of work had been done prior to the advent of nuclear power plants, a great deal of additional research was needed to meet the needs of the nuclear industry, particularly in connection with boiling water

reactors. The experimental boiling water reactor is an outstanding example of a plant whose performance was significantly improved on the basis of new studies on two-phase flows. Originally designed to be operated at 20 MW, the thermal power of EBWR has been more than tripled because of the better understanding of two-phase flow phenomena[2].

In boiling water reactors, subcooled water enters at the bottom of the reactor, boils as it flows along the fuel assemblies and emerges at the top as the steam-water mixture which is single component two-phase flow. The presence of steam bubbles at fuel-water interface is an important characteristic of this type of reactor. It influences not only its nuclear properties but also its thermal and hydraulic performance. It affects the maximum allowable heat flux which in turn may lead to burnout or failure of the fuel clad. It also affects the local value of neutron flux or power distribution.

In a tank type reactor the fuel assemblies are arranged in parallel and experience the same pressure drop from the top to bottom of the reactor core. The flow through each fuel bundle depends upon this pressure loss and in particular upon its two-phase pressure drop component.

The steam volume fraction affects boiling water reactor economies in two ways. For example, a 10% error in

local steam volume produces a change in power distribution of about 2% . Again if it is possible to raise the steam volume in a boiling water reactor without affecting its operability, substantial saving would be made in the costs of the recirculating system. So analytical and experimental studies of the cross-sectional distribution of steam and water are needed in forced convection flow which is very important link in our basic understanding of two-phase flow.

The pressure across the core of a boiling water reactor consists mainly of two-phase pressure losses preceeded by single phase losses at the core inlet. The two-phase pressure losses consist of four components :

(a) hydrostatic pressure losses produced by the variation of coolant density in the axial direction,

(b) acceleration losses. As water is converted into steam, the steam velocity increases giving rise to a loss in head,

(c) frictional losses along the fuel channel and fuel rods

(d) contraction and expansion type losses at spaces and tie plates.

Frictional losses account for major core pressure drop and in this sense it controls any economic role that pressure drop has in boiling water reactor costs. Inaccurate pressure drop values affect the plant performance in two ways. An error in predicting pressure losses produces an

error in total flow across the core and in pumping horse power. It also means that the flow rate within fuel elements is not accurately known. This in turn influences the steam quality in the hottest channel and its margin from the critical heat flux curve.

The other application of two-phase flow in nuclear reactors is Fog-coolant Technology. Fog flow is a term applied to two-phase flow under conditions which cause a large part of the liquid phase to be in a dispersed state within the vapor. This type of flow is characterised by a high vapour volume fraction of the order of 60% or higher and high vapour velocities $>$ 7 meter/sec . Heat removal with this type of coolant flow is achieved by the evaporation of liquid at the heated channel walls and the rapid replenishment of this liquid by turbulent transport of liquid from the bulk of the flow.

Inherent attractiveness of fog as a reactor coolant comes from its low neutron absorption, favorable heat transfer properties and capability of direct cycle operation. It promises to permit direct cycle light water evaporation in high neutron economy reactor systems, and promises extension of boiling water reactor technology to regions of high exit quality and reduced water recirculation rates.

The termsfog flow, dispersed flow, mist flow and steam water spray are some times used to describe what is

meant to be the same kind of flowing vapor-liquid mixture. Actually fog flow implies that all the liquid is dispersed in the vapour phase. But here dispersed flow means vapour-liquid duct flow in which most of the liquid is in a highly dispersed state within the vapor while the remaining liquid, when present, flows as a thin discontinuous film along the duct walls.

The size of the droplets dispersed in the vapor depends on the temperature and mass velocity of the two-phase flow. For steam-water dispersed flow at 71.25 kgf/cm$^2$ abs. and 4.8 x 10$^6$ kgm/hr-meter$^2$ average droplet size is estimated to be of the order of 20 to 40 $\mu$ with a maximum droplet diameter of about 100 to 200 $\mu$ [3]. Under adiabatic conditions the channel walls are believed to be covered with thin flowing liquid film. As heat is transmitted to the coolant through the channel walls the liquid film is believed to break up and disappear near or above the critical value of heat flux, known as the burn out. Below the point of critical heat flux, heat transfer coefficients of 40650 to 81300 kcal/hr-meter$^2$ are obtained by virtue of high mixing in the bulk of the flow and the thin liquid layer at the wall which are characteristic of dispersed flow.

Some of the advantages of using fog flow for reactor cooling are common to boiling water; others are unique to this coolant. The main advantages of this coolant are

summarised by Silvestri[4] as follows :

(i) Coolant density is much lower

(ii) Thermal stresses are reduced since heat transfer to the coolant is by a constant temperature process.

(iii) Very high heat transfer coefficient is possible.

(iv) Direct cycling of coolant into the turbine is possible.

Fog may find application in graphite moderated reactors because of its good cooling properties compared with those of gases. It may find application in fast reactors where minimum moderation is required in combination with high heat transfer[5]. Some of the problems which arise in fog-cooling are listed below[4] :

(i) If fog is not produced at the inlet of each reactor channel, uniform dispersion of the coolant is not possible.

(ii) Steam circulation pumps are required even though the system is direct cycle.

(iii) Coolant velocity 20-34 meter/sec may pose an erosion problem.

(iv) Stability of coolant depends on its quality and flow rate.

(v) At low quality and/or low flow rate the coolant flow pattern changes from a uniformly dispersed mixture to "annular flow" with the bulk of the liquid flowing near the wall.

Dryout and Burnout Conditions :

In steam-water mixture flow there is a precise point at which a more or less rapid surface temperature rises from a temperature close to the saturation value. This condition is known as "initiation of liquid deficiency" or the dryout point. The heat flux which causes this condition is termed as "dryout heat flux". Thus "dryout" of the heating surface causes the "liquid deficient region"(6). Heat flux of the order of $1.355 \times 10^6$ kcal/hr-$m^2$ is required to initiate "dryout" resulting in much lower temperature differences of about 120°C. The heat transfer coefficient is of the order of $4.88 \times 10^3$ to $14.64 \times 10^3$ kcal/hr-$m^2$°C. The "dryout" very seldom leads to damage of heating surface and for this reason the process is some times called "slow burnout".

Departure from nucleate boiling in the subcooled and low steam quality areas causes the process of "film boiling" to be initiated. An insulating vapor film covers the heating surface through which the heat must pass. The heat transfer coefficient is lower than in the dry out condition. It is mainly due to the lower thermal conductivity of the stagnant steam layer. Such a condition is known as burnout. Typical values of the heat transfer coefficient in this region are in the range 146.4 to 1464 kcl/hr-$m^2$ °C with extremely high temperature difference ( $>$1650 °C), Wallis(3). Failure of the heating

surface due to melting or rapture usually occurs. "Burnout" shows a good reproducibility and a regular trend. But to predict burnout with the same accuracy with which heat transfer coefficients are predicted is not an easy task (3).

1.2 Two Phase Flow Description :

The term "two-phase flow" is considered here to be representative of the simultaneous flow of liquid and gas in closed conduit. Upward flow in a vertical conduit is the configuration investigated in this work. The flow pattern in horizontal system will be considered for comparison only. Two general categories are present in two-phase flow studies. One in which liquid and vapor are the same fluid i.e. single component flow and one in which liquid and vapor are dissimilar fluids i.e. two-component flows.

The magnitude of Reynold's number is sufficient to identify the laminar or turbulent type of flow in the case of single-phase flow. In the case of two-phase flow, in addition to type of flow like laminar and turbulent flow, the flow-regimes also come into picture. These flow regimes are not readily described by one or more measurable parameters. Collier's (6) representation of the regimes in two-phase single component flow has been shown in Fig. 8 depicting most of the possible flow regimes in upward co-current vertical two-phase flow in terms of a single tube boiler fed with subcooled water and

producing superheated steam. The walls are subjected to a constant heat flux. The diagram is largely selfexplanatory.

The majority of two phase flow studies have involved water as the liquid and air has been vapor or gas. Two distinct fluids with different properties may flow around each other in a variety of ways which gives rise different flow regimes. Therefore it becomes necessary to recognise the flow regimes before any analysis is to be done.

The description of two-phase flow regimes given by different investigators is not same. For example the survey of literature before 1960 made by Vohr[7] for flow regimes for horizontal and vertical flow gives seven basic horizontal flow regimes. They are as follows :

(a) Bubble flow : This regime is characterised by vapor or gas bubbles which do not completely bridge the area normal to flow.

(b) Plug flow : Long vapor or gas plugs are formed, usually by coolescence of bubbles from the bubble flow. The vapor plugs are separated by liquid plugs which may or may not contain bubbles.

(c) Stratified Flow : The vapor flows in a separated stream above the vapor-liquid interface which remain relatively tranquil.

(d) Wavy Flow : This regime is a continuation of the stratified flow in which the interface develops waves of increasing amplitude.

(e) Slug flow : This regime occurs with a complete bridging of the channel by slugs of liquid which may contain bubbles. This liquid slug traverses the channel at a rapid rate.

(f) Annular Flow : This regime is characterised by an annulus of liquid on the channel walls with the vapor occupying the central region or core.

(g) Spray Flow : The liquid is dispersed in vapor, which becomes the continuous phase. In adiabatic flow it may be expected that the liquid forms patches on the walls if wetting occurs.

Vohr listed the following flow regimes in vertical flow :

(a) Bubble Flow : Vapor bubbles aided by buoyancy effects move through the liquid stream which is considered to be the continuous phase.

(b) Piston Flow : The vapor forms long plugs with a rounded leading surface. The liquid plugs that separates the vapor plugs may contain entrained bubbles.

(c) Semi Annular, dispersed Plug Flow, emulsion flow, turbulent flow, slug-annular flow : These various terms have been used for regimes that separate the piston flow regime from the fully developed annular

regime. The flow structure is random in nature with both phases alternately attempting to assume the continuous form.

(d) Annular Flow : This regime is characterised by an annulus of liquid on the channel walls with vapor occupying the central core.

(e) Spray or dispersed Flow : The liquid appears in droplets or ligament form and is dispersed in the continuous vapor phase.

By way of contrast, the classification made by Nicklin and Davidson[8] for vertical flow in air water systems is as follows :

(a) Bubble Flow : The bubbles are small in comparison with the flow area and the shape is not greatly affected by the confining walls.

(b) Slug Flow : The bubbles appear as in elongated forms, which have a rounded leading surface and a nearly flat bottom. The length varies by as much as several hundred tube diameters. These vapor slugs maintain their identity as they move up the conduit.

(c) Semi annular Flow : This regime has an appearance similar to the slug-flow regime in that alternate slugs of liquid and gas occur. However the liquid regions alternately tend to build up and break down which results in churning motion.

(d) Annular Flow : The liquid is maintained on the walls, and the gas flows in the core. The interface is wavy, and the amplitude of the waves is not sufficient to form a liquid bridge.

(e) Mist Flow : The liquid is carried in the form of droplets swept from walls by the gas flow.

Martinelli et al[9] made a distinction between various possible flow mechanisms by considering the laminar and turbulent flow possible for both the gaseous and the liquid phases. In this way it is possible to have four flow mechanisms. Superficial Reynold's numbers of the phases are taken as the characterising parameters. This classification of flow mechanism was successfully used by them in the analysis of two-phase pressure drop. However its applicability to other aspects of two-phase-flow is not known.

The transition between flow regimes means that a small set of conditions exists in which the distinction between two adjoining regimes is indeterminate. Again two sets of conditions bound this set such that each set is identifiable as a particular regime. The statement of a flow regime transition may be made on the basis of the mean value of a transition set, the upper bound or the lower bound. The representation of all possible transitions on a single plot or map in terms of two parameters would be most desirable

for all fluids and all operating conditions. Separate plots are also required for a system in which the two phases are injected separately and for systems in which the fluid undergoes a transformation of phase by heating. A general map covering all possible situations in two-phase flow will probably not be developed until transitions between regimes are well established.

## II REVIEW OF LITERATURE

This section summarises the nature of previous work on two-phase flow which is closely related to this work. The literature in two phase flow studies is quite extensive as can be seen from the recent annotated bibliographies by Robert et al[1] and Gouse[7].

Moore and Wilde[2] carried out a series of experiments to study gas slippage in vertical tubes using water, kerosene and three different oils. They concluded that the surface tension of the liquid has a definite influence on the slip ratio.

Somissaret[2] studied two-phase flow parameters for upward co-current vertical flow in air-water, nitrogen-Freon-113 and nitrogen-mercury mixtures. Tests were performed in a natural-circulation loop at atmospheric pressure. The superficial water velocity ranged from 0 to 0.3 meter/sec; air weight fraction ranged from 0.0125 to 0.100. The studies of air-water flow was made in a 7 cm. I.D. test section. He concluded that two-phase flow parameters changed significantly with superficial liquid velocity and air-weight fraction in this low circulation range. Slip ratios were found to be directly proportional to the surface tension of the liquid and inversely proportional to the dynamic viscosity of the liquid.

2.1 Gazley[10] based on experimental evidences has pointed out that pressure drop in two-phase flow is affected by the types of flow regimes.

Lockhart-Martinelli[11] have proposed a correlation for pressure drop calculation based on certain limiting assumptions. These assumptions are :

(i) The static pressure drop for gas phase is equal to that of liquid phase, regardless of flow patterns.

(ii) Volume occupied by the gas plus that occupied by liquid at any instant equals the pipe volume.

(iii) Four types of flow patterns were recognised consisting of the four combinations possible with either phase being considered in turbulent or viscous flows.

The results have been presented as a plot of a function $\phi$ against a parameter X, with one curve representing each of the four flow patterns. This correlation was originally based mainly on data obtained for isothermal horizontal flow at atmospheric pressure and normal temperature in 2.54 cm. dia pipe using air and eight different liquids.

The correlation quantities are defined as

$$\phi_g^2 = \frac{(\frac{\Delta P}{\Delta Z})_{TPF}}{(\frac{\Delta P}{\Delta Z})_G} \quad \text{or} \quad \phi_L^2 = \frac{(\frac{\Delta P}{\Delta Z})_{TPF}}{(\frac{\Delta P}{\Delta Z})_L}$$

$$\text{and } X^2 = \frac{(\frac{\Delta P}{\Delta Z})_L}{(\frac{\Delta P}{\Delta Z})_G} .$$

In this correlation the pressure drop during two-phase flow is related to the pressure drop occuring if only a single phase flowed in the conduit. This correlation has been applied to all regimes of two phase flow both by the originator and by many other investigators. Isbin et al[12] checked the correlation experimentally and found that it deviates by nearly ± 50% in predicting two-phase flow pressure drops and that it also depends on the liquid flow rate. Collier and Hewitt[13] showed that the predictions of this correlation of frictional pressure drops for vertical turbulent-turbulent flow are too low for $X < 10$; but are satisfactory for $X > 10$ for air water flow in small diameter tubes.

Davis[14] presented a modified Lockhart-Martinelli method based on Govier's[15] data. He suggested that the introduction of Froude number into the Lockhart-Martinelli parameter X takes account of gravitational and inertial forces, so that the model can be applied to vertical flow. The revised parameter X is defined for turbulent-turbulent flow as

$$X = 0.19 \left(\frac{W_L}{W_G}\right)^{0.9} \left(\frac{\rho_G}{\rho_L}\right)^{0.5} \left(\frac{\mu_L}{\mu_G}\right)^{0.1} \left(\frac{V_m^2}{g\,D}\right)^{0.185}$$

When results predicted by this method are compared with other data, a deviation of ± 20% is found for liquid Reynold numbers above 8000 if the Froude number exceeds 100.

Sofer[5] correlated frictional pressure drop data under dispersed flow conditions of steam-water flow using the homogeneous flow model. He employed an empirically modified Reynolds number $R_m = \frac{DG}{\bar{\mu}} \left(\frac{G}{1.77 \times 10^6}\right)^2$. Then

$$\Delta P = 2 f \frac{L}{D} \bar{v} G^2 + (\bar{v}_o - \bar{v}_i) G^2$$

and $$f = 0.046 R_m^{-0.2}$$

where $$v_o - v_i = v_{fg} (x_o - x_i)$$

$$\bar{v} = x v_g + (1-x) v_f$$

$$\bar{\mu} = x \mu_g + (1-x) \mu_f$$

He found good agreement between this equation and data obtained for adiabatic fog flow in round tubes.

Lockhart-Martinelli correlation was further extended by Martinelli and Nelson[14] for steam-water flows. The correlation is in terms of $\phi_o^2$ vs. quality, the pressure being a parameter. Sharma et al[16] experimentally investigated pressure drop for steam-water fog flow in vertical channel. They used a round tube of 2.54 cm. O.D. and an annulus of 2.54 cm. O.D. and 1.27 I.D. Parameter ranges studied are pressure 6 kg/cm$^2$ abs. to 7 kg/cm$^2$ abs, mass velocities $10^6$ kg/hr-m$^2$ to 1.3 kg/hr-m$^2$, and qualities 0.4 to 0.6. They concluded that for low pressure fog-flow the Martinelli-Nelson correlation gives pressure and vapour volume fraction to an accuracy of 20 to 30%. They

also pointed out that there is a definite dependence of the pressure drop parameter $\phi_{Lo}^2$ on the mass velocity of flow and the geometry at given values of pressure and quality.

2.2 Regime Transition in two-phase flow

A number of attempts have been made to prepare charts which would allow prediction of the state of flow from a knowledge of flow variables. Such charts usually take the form of a set of curves outlining regions in which various flow regimes might be expected to occur. One such chart has been presented by Johnson and Abou-sabe[17]. They defined flow regimes by plotting liquid superficial mass velocity against gas superficial mass velocity. Hoogendoorn[18] used the volumetric fraction of the gas as ordinate and the mixture velocity as abscissa.

The principal flow regime map in horizontal flow is due to Baker[19] who utilised data from various investigators mainly air-water systems to develop his flow map as shown in Fig. 7. He plotted gas-mass-velocity against the liquid-to-gas mass velocity ratio of the feed. Correction factors for fluids of different densities, viscosities and surface tension were introduced in an empirical way. The coordinates of Baker's map are

$$\frac{G_g}{\lambda} \quad \text{and} \quad \lambda\psi\left(\frac{G_l}{G_g}\right)$$

where $\lambda = \left[\left(\frac{\rho_g}{0.075}\right)\left(\frac{\rho_l}{62.3}\right)\right]^{1/2}$

$$\psi = \left(\frac{73}{\sigma}\right)\left[\left(\frac{\mu_L}{1}\right)\left(\frac{62.3}{\rho_L}\right)\right]^{1/3}$$

The numerical factors in Baker's parameters are identified as

0.075 = density of air at standard pressure and temperature lbs/cft

62.3 = density of water at room temperature lbs/cft

73 = surface tension of water at room temperature dynes/cm.

1. = viscosity of water at room temperature C.P.

Although the border between two regimes shown in this map are lines, in reality these borders are rather broad transition zones.

Goldmann (30) et al have converted Baker's plot to plots for an adiabatic steam-water system. The coordinates for the map were the total mass flow rate and the quality. The presentation of flow regimes in this form confines the results to a single pressure. Thus a family of transition curves would be necessary to display the effects of system pressure.

Some investigators have assumed that the effect of gravitational acceleration at very high flow rates is negligible. They have also assumed that in such cases vertical flow-regimes are similar to the horizontal flow regimes. Thus at high flow rates Baker's map and Goldmann's map can be used for vertical flow too.

Nicklin[21] has suggested the requirement for stable idealised annular flow where all the liquid flows in the wall film as follows :

(i) The forces on the film must be in equilibrium.

(ii) The net flow of liquid and gas at any section must equal the respective flows entering the tube.

(iii) The relative motion of the phases must create an interfacial shear stress compatible with (i).

(iv) The film must be stable to local thickening or thinning.

(v) There must be some way of developing the film initially.

Sekoguchi et al[21] have pointed out that some regimes in two-phase flow may not exist in very short test section because of the time required for a particular regime to form.

The transition behaviour from one regime to another has not been well established. Govier[22] summarised test results in vertical two-phase flow for the transition of various flow regimes.

Moissis[23] developed a transition criteria from slug to homogeneous flows by equating the relative velocity of the vapor slug and the liquid flow. His conclusions are as follows :

(i) Since in a given two-phase flow bubbles of various lengths may exist, the transition cannot be defined in terms of a line but can only be bounded within a band.

(ii) The transition depends on the size of the bubbles in the slug flow. At the same quality a system consisting of long bar spaced bubbles is more stable than one consisting of short closely spaced.

(iii) Increasing the pipe diameter accelerates the transition process.

(iv) Increasing the Weber number accelerates the transition process.

Rossum[24] examined the transition from annular flow to annular with droplet entrainment experimentally. He mainly studied the variation of surface tension and viscosity of the fluids in a rectangular duct. Minimum gas velocity for entrainment was found to be proportional to the surface tension and given by $V_* = c_1 \sigma$ . The value of c was 0.82 for horizontal and 1.25 for vertical downward flow when $V_*$ was in ft/sec and $\sigma$ in dynes/cm.

Sagar et al[25] made visual observation of structural forms of the flow in vertical annuli with equivalent diameters of 0.0232, 0.0141 and 0.0061 meters at close to atmospheric pressure. They established experimentally the transition criteria of flow regimes. They used air-water two-phase flow. The experiments to determine transition from one regime to another were carried out with constant water-flow rate while the air flow rate was changed within the limits which produces all possible structures. They

established a relation

$$\beta = f\,(F_{r_{mix}}) \text{ where } F_{r_{mix}} = \frac{w_{mix}^2}{gD_{eq}}$$

$$w_{mix} = w_o'' + w_o'$$

$$\beta = \frac{w_o''}{w_{mix}} = \text{volumetric void fraction.}$$

They plotted $\beta = c\,(F_{r_{mix}})^n$ and found that $\beta > 0.8$ and $60 < F_{r_{mix}} > 2$ for annular-dispersed flow. They also determined from the plot that c varied from 0.6 to 0.83 and n from 0.06 to 0.04 for annular-dispersed flow transition.

Kremnev et al[26] studied the heat transfer behaviour in a two-phase dispersed flow. They used different terminologies for the same regime, for example Fog flow, dispersed-annular flow, spray-flow or fog with wetted wall. They produced this regime with air superficial velocity from 20 to 48 m/sec and moisture content from 35 to 80 gms. per cubic meter of air. A plot of gms. of water per cubic meter of air vs. superficial air velocity has been presented which is a straight line.

## 2.3 Photographic Studies

Wallis[3] presented a paper which describes experiments in which air was blown through the walls of porous tube submerged in water. He observed three different flow patterns, bubbly, patchy and blanketed. He used moving pictures at 3000 frames per second and succeeded in providing a clear picture of the flow patterns.

Carter and Huntington[27] studied concurrent vertical upward flow of air and water in a 2.1/8" x 20 ft open transparent tenite tube as well in a 5/16" x 2.1/8" annulus. They used normal and high speed motion pictures which made it possible to see flow mechanism indistinguishable to naked eye.

Alves[28] did photographic study of flow regimes. He took photographs of typical flow regimes using the glass observation section. Diffused light was passed through one side of the section and photographs were taken from the opposite side with an exposure time of 1/1000 second. With air-water horizontal flow, the annular flow occured at superficial air velocities of 6.5 m/sec to 23 m/sec depending upon the liquid rate. For superficial liquid velocity greater than 1 m/sec, it was difficult to distinguish annular flow from bubble flow by visual observation. His conclusions are flow regimes depend upon the liquid and gas flow rates and also upon the type of inlet.

A direct two-colour lighting system has been suggested[8] which produces a positive distinction between the two-phases.

## 2.4 Comments on Earlier Studies

The graphical representation of flow regimes by Hoogendyoom[18] is not convenient. He used the volumetric fraction of the gas as ordinate and the mixture velocity as

abscissa. The important ranges of flow regimes tend to be squeezed together in small area of the plot. Plots given on weight basis yield a more equitable arrangement of flow regime-areas than those on volume basis.

Wallis[29] tested the homogeneous model for pressure drop prediction. In all cases it was found that homogeneous theory gave better estimate of frictional pressure drop than Martinelli's correlation in annular-dispersed flow.

Sharma et al[16] compared Martinelli's correlation and Homogeneous model for frictional pressure drop in fog flow. It was found that Martinelli's correlation was in better agreement with experimental data than that of Homogeneous model.

Most of the work reported has been done in restricted ranges of gas or liquid flow rates, fluid properties and pipe diameter so a general deduction is not possible. The effect of the change in fluid properties and dia of the conduit has not been well defined.

One of the principal objective of these visual flow studies has been that of obtaining a clean picture of the flow regimes. Unfortunately the written word or even a series of still photographs cannot convey adequately the visual story to the reader of a published page. A large number of photographic observations have been made. The methods used include still pictures, motion pictures, and X-ray

pictures. But carefully taken still pictures also show a lot of detail and serve as the standard for flow regime definition. The best observations can be obtained by utilising a microscope for viewing the regimes.

## III DESCRIPTION OF THE EXPERIMENTAL SET UP

### 3.1 Brief Summary of Equipment and Operation

The proposed study of the transition from dispersed flow to annular flow in two-phase water-air system was done in a vertical channel. Depending upon the available compressor capacity the test section was cho sen in such a manner that dispersed flow could be achieved in the existing conditions. The set up was designed and fabricated partly in the Nuclear Heat Transfer Laboratory and partly in Refrigeration-Airconditioning Laboratory.

3.1.1 A rough design for cross section of the test section was made based on Baker's plot. The cross section was then actually tested to see whether dispersed flow was developed or not. Finally a circular pyrex glass tube of 11.5 mm I.D. and 16 mm O.D. was chosen. The length available was limited to 1400 mm. Two pressure taps were inserted into the test section as located in Fig. 2. A calming length equivalent to 35 diameters i.e. 400 mm of the tube was allowed between the tube inlet and the lower pressure tap. This was done to prevent upstream disturbances. The upper pressure tap was inserted 200 mm below the upper end of the tube in order to prevent down stream disturbances. Thus a test length of 800 mm was provided between the two pressure taps. The

lower end of the test section was connected to a brass fitting as shown in Fig. 3. This end connection was designed and fabricated in Fabrication Shop. The upper end of the test section was connected to a 1.27 cm. G.I. pipe with a flexible joint which exhausts the air-water mixture to the atmosphere. The test section after assembly was made peffectly vertical with the help of a plumb line.

3.1.2 Air Supply

Three air compressors at discharge rate 11 cFM, 8.3 cFM and 5 cFM and at maximum pressure of 200 psi were used. These compressors are of K.G. Khosla make and the connections are shown in Fig. 1. In order to reduce the relative humidity a simple air dryer was designed, fabricated and connected in the air line of the set up as shown in Fig. 1 and 20. Air was passed through three beds in series. First it was passed through a gravel-bed which was put in an U-Tube made up of 3.175 cm dia. polythene tube. Then it was passed through a straight horizontal section filled with cotton waste and finally it was passed downward through a column of silica-gel. An ordinary thermometer was inserted in the upstream of the orfice meter range 0 to 50°C least count 0.2°C. A humidditymeter was used to test the R-H of the air after the dryer.

3.1.3 Water supply

Ordinary tap water was used directly. A dye storage compartment was connected in the line in order to introduce a green solid dye into the test section when required.

In order to mix water and air uniformly and continuously a mixing chamber was designed and fabricated as shown in Fig. 1, 5, 6 and 22. The unit consists of a conical chamber, an entry port for air and an atomiser. The atomiser as shown in Fig. 4 is used for spraying the incoming water. Some atomisers of different hole-diameters were designed and fabricated in the Precision Shop. On trial and test basis one atomiser was chosen for this work. This could give a spray of water even at the minimum water flow rate.

3.2 Instrumentation and Measurements

The aim of this experiment was to study the transition from dispersed flow to annular flow. There is a wide choice of variables for studying this particular phenomenon. The final selection of variables was based upon ease of measurement and the availability of equipment . The variables that were to be measured during the operation of the experiment were mass flow rate of air and water, the inlet pressure of the test section and the pressure drop in the test section. Because of the limitations of the pressure obtainable

from the compressor the study was confined to these values of pressure, viz. 1.1736, 1.3142 and 1.5954 kgf/cm$^2$ abs. At these three pressures, mass flow rates were the variable parameters. Ultimately the experimental parameters are the pressure at the inlet of the test section and the mass flow rates of air and water. By varying these three parameters, many different operating conditions were achieved. These parameters were chosen since the particular regimes of the two-phase flow studied strongly depend upon mass flow rates of air and water.

For air flow measurement an orficemeter was designed and fabricated according to ASME specifications. The details are given in the appendix. For water flow measurement a rotameter of range 0.05 to 0.55 gpm and least count 0.01 gpm was used. [The errors in measurement are given in RESULTS, DISCUSSSION AND RECOMMENDATIO The rotameter was actually calibrated using a measuring flask & a stop watch.]

One Heise pressure gauge (range 0 to 100 psi and least count 0.1 psi) was used with the orficemeter. Another Heise pressure gauge (range 0 to 50 psia and least count 0.1 psi) was used to measure the pressure at the inlet of the test section. A third Bourdon's compound pressure gauge was used to measure the pressure of water entering the test section.

A Dwyer manometer (range 0 to 24 inches of water and least count 0.1 inch of water) was used across the orficemeter. Another mercury manometer (range 0 to 12 inches

of Hg and least count 0.1 inch of Hg) was used across the test section. Both the manometers were used for differential pressure measurements.

Needle valves were used to control the flow of air and water. At other points globe valves were used. A pressure reducing valve was used in the air line before orficemeter, in order to keep air pressure at the inlet of the test section constant irrespective of the discharge. A non return valve was fitted in the air line after the orfice meter to prevent water contamination with fluid of Dwyer manometer.

The set up was made free of vibration by connecting the compressor outlet and the air lines by means of a high pressure flexible rubber tubing. Precautions were taken to prevent the compressors from overheating.

## 3.3 Experimental Procedure

Initially, the water rotameter was calibrated with the help of a measuring flask and a stop watch. The compressors were started. The water inlet valve was opened and the water filled the test section and manometer legs. The water valve was closed and air was allowed to pass through the test section. In this operating condition all joints were checked for air leak with the help of soap solution. Then all the joints in the set up were made

leakproof. A test run of the operation was made by allowing air and water to flow together in the test section. After that the water flow was stopped and air flow continued till the test channel became dry. Then the air was stopped and the zero readings of the instruments were noted.

The inlet pressure to the test section and the discharge of air were set to particular values and the air was allowed to pass through the test section. Then a small amount of water was admitted to the mixing chamber. After some time dispersed flow was observed in the test channel. The amount of water was increased slightly in steps of 0.005 gpm. At the same time the drain off valve was also controlled in order to remove excess water in the mixing chamber. After every step increase in water flow for a fixed value of air, about 5 minutes were allowed to make the flow steady. The arrangement of drain-off valve has been shown in Fig. 5, 6 and 22. The drain off valve was connected with a polythene tube to the mixing chamber. A constant level of water was maintained by controlling the drain off valve. Thus water acts as a seal to prevent air leakage through the drainage valve.

After increasing the water flow step by step it was found that dry dispersed flow changes to wet dispersed regime. Finally for a particular water flow, the flow

became completely annular. At this particular stage the orficemeter readings, water rotameter readings and the drained off water rate were noted. The pressure drop in the test section was also noted for the particular condition. After noting all the readings the water supply and the air supply were stopped. The zero error of the instruments was noted. Again for the same inlet pressure at the test section, the discharge of air was set to a lower value and with the help of the pressure reducing valve the inlet pressure at the test section was brought to the original one. The previous steps were repeated until the transition from dispersed to annular flow took place. At this instant the second set of readings were noted. In this way for the particular test section inlet pressure and for different air flow rates, the quantities of water flow required to obtain transition from dispersed flow into annular flow were obtained. In this way three inlet test-section-pressures were used to obtain three sets of readings, each set corresponding to about six air flow rates.

The regimes observed during the main experimentation were verified by adding a very dilute green dye to the water. The readings obtained in this case for a particular condition was same as in the main experimentation.

3.4 Photographic Equipment and Technique

Here the still picture technique was adopted. Unfortunately even high speed motion pictures have not clarified the transition from one regime to another(8). In the present photographic study a technique of diffused light was used. Three sides of the test section were covered with tracing sheets. The fourth side was exposed to the camera. Illumination was provided on the two sides using one bulb of 500 watts each side. On the third covered side day light was allowed to shine as shown in Fig. 6(a). In this way diffused light on the test section from three sides were used. The camera was kept at 0.3 meter from the test section and a close up attachment was used.

The experiment was run at 1.3142 kgf/cm$^2$ abs. of the inlet test section pressure. A very dilute green dye was introduced to the water. Table No. 4 represents the air flow rates and water flow rates at the conditions where photographs were taken. Photographs for increasing water rates and keeping air flow rate constant were taken. Then some phtographs were taken by decreasing air flow rate in order to study transition from annular flow regime to plug flow regime. A 35 mm INDU film was used. The exposure time was 1/500 seconds.

# IV RESULTS, DISCUSSIONS AND RECOMMENDATIONS

## 4.1 Results and Discussions

The results of the present investigation are presented in the form of graphs, photographs and tables.

### 4.1.1 Flow Regimes

Flow regimes observed in the test section were recorded along with the entrance pressure by still photographs. A series of the photographs were taken starting from dispersed flow till it became just annular. Photographs were also taken for plug flow. It was found that the actual flow regimes encountered depended upon the magnitude of the mass flow rate and the initial fluid conditions.

In the case of annular flow the walls of the conduit are covered by a film of liquid while the central core contains air and possibly some entrained water drops. The character of the liquid film varied from a slow-moving liquid with small waves on the interface to a highly disturbed surface on which both small waves and faster moving high amplitude waves existed simultaneously. Two types of annular flow were observed. The first one can be named as unsteady-annular regime which could develop just after the transition from dispersed flow. In this case there was fluctuation of manometer readings. The next observed regime was steady-annular flow. In this case there was no fluctuation of manometer readings.

Two types of dispersed flow were observed. The first one was the dry-dispersed-flow in which there were no strips of water-film on the walls of the channel. The second one was the wet-dispersed-flow in which there were water-film strips on the wall of the channel. In dry-dispersed flow almost all the water drops were entrained in the air core. In wet dispersed flow the strips were regular and then became unsteady just before the transition to the annular regime.

The inlet conditions are important. If water is injected smoothly on to the walls of the channel, there is no immediate entrainment of the droplets in the core even when flow rates are high. Time and length are required to establish the wave pattern or other film instabilities which allows the droplets to form and mix with the gas in the core. When the water is injected as spray, it is redeposited on the walls eventually setting up an equilibrium condition. If water is not injected as spray this equilibrium may require a thousand or more diameters to establish itself.

4.1.2 Extension of Baker's Plot

The principal flow-regime map in horizontal flow is due to Baker[19]. Fig. 7 shows the original map due to baker. Some investigators have considered the effect of gravitational acceleration at very high flow rates to be negligible and so the vertical flow regimes would be

similar to the horizontal forms. The coordinates in the Baker's plot eliminate the difference between pipes of different sizes. The limits of coordinates used in the Baker's plot are $(\frac{G_l}{G_g})\lambda\psi$ from 1 x $10^{-1}$ to $10^5$ and $\frac{G_g}{\lambda}$ from $10^2$ to $10^5$. No investigation has been done for $(\frac{G_l}{G_g})\lambda\psi$ less than 0.1.

Here a similar plot has been presented based on the present investigation as shown in Fig. 9. In this work the boundary between dispersed and annular flow has been presented for $(\frac{G_l}{G_g})\lambda\psi$ from 3.3 x $10^{-2}$ to 0.1.

The readings were taken at three different inlet pressures to the test section. Nothing can be concluded in general for the effect of inlet pressure due to small number of readings. But it can be concluded that for the same air flow rate, as the inlet pressure increases more water is required in order to obtain a transition from dispersed flow to annular flow. Since all the readings were taken visually, a sharp boundary between the two regimes cannot be drawn. The upper part represents the dispersed regime whereas the lower part represents annular regime. The points represent the observed state points for transition for a given pressure.

4.1.3 Extension of Goldman, Firstenberg and Lombardi-Plot

The applications of the generalised Baker's plot to steam and water data at elevated pressure are made by Goldman et al[30]. In their work the co-ordinates for the map are total mass flow rate and quality. In the present work a similar plot has been made in Fig. No. 10. Here total mass velocity and air weight fraction are taken as coordinates of the plot and the inlet pressure as parameter of the plot. This plot has been deduced from Baker's plot for the parameters of the present work. From this plot it can be concluded that as air weight fraction decreases, the transition from dispersed to annular flow takes place at lower total mass velocity for the same inlet pressure. At the same time as the inlet pressure increases at a given air-weight fraction a higher value of total mass velocity is required in order that transition takes place from dispersed to annular flow.

4.1.4 Kremnev et al-Plot

Kremnev et al[26] have presented a plot for the dispersed flow regime in which the mass of water per unit volume of air and the superficial gas velocity are used as the coordinates. A similar plot for transition from dispersed to annular flow is shown in Fig. 11 in which the data from the present work are used. The work of Kremnev et al has been

compared with present work.

4.1.5 Photographic Work

Between the regions of dispersed and annular flow there is a wide transition band. Whatever be the method of measurement used to define the regime transition, there would still be a band where there would be a question as to whether one should call the flow annular or dispersed flow. In the present work the readings were taken where the flow becomes just annular as per visual observation. So the line of demarcation in Figs. 9, 10 and 11 represents a line in the transition band only.

Visual observations were recorded by means of still photographs. The series of photographs are shown in Fig.13 to 18. These phtographs are the records of flow patterns at 1.3142 kgf/cm$^2$ abs. test section inlet pressure and at different superficial velocities of air and water. Fig.13(a) represents the pattern of dry dispersed flow when $V_{gs}$ is 47.8 m/sec and $V_{fs}$ is 0.8 mm/sec. Fig. 14(b) represents the pattern of wet dispersed flow where $V_{gs}$ is 47.8 m/sec and $V_{fs}$ is 1.44 mm/sec. Fig. 15 represents the transition where dispersed flow disappears and annular flow starts. In the present work Fig. 15(b) records the transition from dispersed flow to annular flow for which all readings were taken. Fig. 16(a) shows the annular flow with indicated velocities.

Transition from annular flow to plug flow has been also recorded by means of a few photographs: Fig. 16(b) to 18(a) records the transition from annular flow to plug flow. Fig. No. 18(b) represents the plug flow where $V_{gs}$ is 14.95m/sec. and $V_{fs}$ is 2.64 mm/sec.

4.1.6 Pressure Drop Data

Table No. 1, 2 and 3 show the pressure drop data in two phase flow along the unheated circular test section for three entrance pressure viz.1.1736 kgf/cm$^2$ abs, 1.3142kgf/cm$^2$ and 1.5954 kgf/cm$^2$ abs and for different mass flow rates. These data show the pressure drop in a circular test section when transition is taking place from dispersed regime to annular regime. Fig. 12 shows the plot of pressure drop vs. air weight fraction taking entrance pressure as parameter. Here it is seen that as entrance pressure increases pressure drop increases. Also for the same entrance pressure, pressure drop increases as air weight fraction increases.

The errors involved in the present work cannot be assessed quantitatively since the regimes were identified by visual observations.

4.2 Recommendation for Future Work

The following recommendations for further investigation are made :

(i) The effect of diameter and geometry has not been established in any of the investigations to a satisfactory degree. It would be beneficial to consider a

fixed external loop and to vary the shape, size and length of the test section. In particular the proper equivalent diameter to be employed for non-circular conduits, must be established.

(ii) X-ray photographs may be utilised to obtain well defined flow regimes.

(iii) A study of flow regimes using optical microscope may yield more definite results regarding flow regime transition.

Errors in measurements : -

The errors can be brought together in three major groups. Errors in measurement of mass flow rates, errors in measurement of pressure drop and errors in distinguishing the regime visually. Other data required in the calculation like densities, surface tension etc. have been taken from standard hand books.

The errors in air flow measurement by orfice meter can be calculated based on least count of measuring instruments i.e. manometer, pressure gauge, thermometer and vernier calliper.

$$\frac{\Delta w_g}{w_g} = \frac{1}{2}\frac{\Delta P_1}{P_1} + \frac{2\Delta D_2}{D_2} + \frac{1}{2}\frac{\Delta h_w}{h_w} - \frac{1}{2}\frac{\Delta T_1}{T_1}$$

where $\Delta P_1 = 0.1$ psi; least count of the pressure gauge

$P_1 = 13$ psi ; minimum pressure

$\Delta h_w = 0.1"$ ; least count of the manometer

$h_w = 1.5"$ ; minimum differential pressure head

$\Delta D_2 = 0.005"$ ; least count of the vernier calliper

$D_2 = 0.485"$ ; dia of the orfice.

$\Delta T_1 = 0.2°C$ : least count of the thermometer

$T_1 = 17°C$ ; minimum temp. of the air

$$\therefore \left(\frac{\Delta W_g}{W_g}\right) = \pm 5.21\%$$

Errors due to non-conformity of the orficemeter with the specification, including dia of the orfice, distance of taps, distance of calming section cannot be estimated accurately. However it is felt that this will be significant. To be on the safer side in error calculation, $\left(\frac{\Delta W_g}{W_g} = \pm 5.21\%\right)$ is multiplied by a factor of 2 which makes $\frac{\Delta W_g}{W_g} \simeq \pm 10\%$.

Similarly the error in water flow measurement can be calculated based on the least counts of the rotameter and the measuring flask and also the error in the observation of time by the stop watch.

$$\frac{\Delta W_1}{W_1} = \frac{\Delta G}{G}\left(1+\frac{F}{Gt}\right) \pm \frac{F}{Gt}\left[\frac{\Delta F}{F} + \frac{\Delta F}{Gt} - \frac{\Delta t}{t}\right]$$

where $G$ = 340 cc./minute ; 0.09 gpm.

$\Delta G$ = 0.00125 gpm; error in rotameter reading observation

$F$ = 320 cc. ; maximum reading in the measuring flask

$\Delta F$ = 2 cc. least count of the measuring flask

$t$ = 1 minute; time of observation

$\Delta t$ = 2 seconds; estimated error in time of observation

$$\therefore \frac{\Delta W_1}{W_1} = \pm 4.3\ \%$$

Maximum error in pressure drop measurement can be estimated based on error due to least count of the manometer and error due to

the shape of the pressure tappings. The estimated value of the error in $(\frac{\Delta P}{\Delta Z})_{TPF}$ due to the shape of pressure tappings is 1.1%.*

Error in $(\frac{\Delta P}{\Delta Z})_{TPF} = \frac{\Delta h}{h} \times 100 + 1.1$

where $\Delta h = 0.05"$ ; error in manometer reading

$h = 1"$ ; minimum pressure drop

Error in $(\frac{\Delta P}{\Delta Z})_{TPF} = 6.1\ \%$ .

This error of 6% is to be used with all the pressure drop calculations reported in this thesis. The error estimates on the flow measurements have been incorporated in Fig. 9 which gives the Baker's plot for the transition. A combination of the errors in $(G_l/G_g)\lambda\psi$ and $G_g/\lambda$ which are the abscissa and ordinates in Fig. 9 shows that the uncertainty in predicting transition of the regime is of the order of $\pm$ 16%. The uncertainty is shown in the case of the 4 psig readings by a hatched area.

---

* Bendick, R.P. "Fundamentals of Temperature pressure and flow measurement", John Wiley and Sons Inc. pp 238 (1969).

# REFERENCES


1. Robert, R. Kepple and Thomas, V. Tung, "Two-phase (gas-liquid) System of Heat Transfer and Hydraulics", An annotated Bibliography, ANL-6734 (1963).
2. Smissarert, George, E., "Two component Two-phase Flow parameters for low circulation Rates", ANL-6755 (1963).
3. Wallis, G.B., "Some Hydrodynamic Aspects of Two-phase Flow and Boiling", International Development in Heat Transfer, Pt. II, pp 319-340, ASME (1961).
4. Silvestri, M. et al, "Fog coolant project", Nucleonics, Vol. 19 (I), pp 86 (1961).
5. Sofer, A. George, "Fog Coolant Technology and its application to Nuclear Reactors", Chemical Engg. progr. symposium series, Vol. 60, Part XI, No. 51, pp 120 (1964).
6. Collier, J.G., "Heat Transfer & Fluid Dynamic Research as Applied to fog-cooled power Reactors", AECL 1937.
7. Gouse, S. William, "An Index to the Two-phase Gas-liquid Flow literature, Jr. M.I.T. Report No. 9 (1966).
8. Baker, James, L.L., "Flow regime Transition at Elevated pressure,", ANL-7093 (1965).

9. Martinelli, R.C. et al, "Isothermal pressure Drop for Two-phase Two component Flow in Horizontal pipe", Trans. ASME 66 (Feb. 1944).

10. Gazley ...., Chemical Engineering Progress, Vol. 45, pp 45-48 (1949).

11. R.W. Lockhart & R.C. Martinelli, "Proposed Correlation of Data for Isothermal Two-phase two-components Flow in pipes", Chemical Engineering Progress, Vol. 45, pp 39 (Jan. 1949).

12. Isbin et al, A.I. Ch. E. Jr., 3, pp 361(1957).

13. Collier, J.G. and Hewitt G.F., Trans. Ins. Chem. Engrs. (London) , 39, pp 127 (1961).

14. Advances in Chemical Engineering, Vol. IV, Academic Press, New York (1963).

15. Govier, G.W., Canadian Journal of Chemical Engineering, 35, pp 58 (1957).

16. Sharma, M.P., Srikantiah, G. and Surya Pratap, V.,"An Experimental Investigation of Steam-water fog flow in vertical channels", First National Heat and Mass Transfer Conference, I.I.T. Madras HMT-46-71(1971).

17. Johnson & Abou-Sabe, Trans. of ASME 74, pp 997 (1952).

18. Hoogendroom; Chemical Engineering Sci., 9, pp 205 (1959).

19. Baker, O., "Simultaneous Flow of Oil and Gas", Oil Gas Jr. 53, pp 185-190 (1954).

20. Goldmann et al, "Burn out in Turbulent-A droplet diffusion Model", Trans. ASME Ser.C.Jr. of Heat Transfer, 83, pp 158-162 (1961).

21. Sekoguchi, K. et al, "The Influence of Mixers, Bends and Exit sections on Horizontal Two-phase Flow", Cocurrent Gas-liquid flow; a symposium of the Canadian Society for Chemical Engineering No. 1.

22. Govier, G.W., "Development in Understanding of the Vertical Flow of two-fluid phases", Canadian Jr. of Chemical Engg. 43, No. 1, pp 3-10(1965).

23. Moissis, R., "The Transition from Slug to Homogeneous Two-phase Flow", Trans. ASME Ser. C, Jr. of Heat Transfer; 85C, pp 366(1963).

24. Rossum, J.J. Van., "Experimental Investigation of Horizontal Liquid Films Wave formation, Atomisation, Film thickness", Chem. Engg. Sci. 11, pp 35-52 (1959).

25. Sagar, I.I. et al., "Structure of Two-phase flows in vertical Annuli at low pressure", Heat Transfer-Soviet Research, Vol. 2, No. 3, pp 128 (May 1970).

26. Kremnev et al., "Heat Transfer in Two-phase dispersed flow", Heat Transfer-Soviet Research, Vol. 2; No. 6 , pp. 100 (Nov. 1970).

27. Cecil, O. Carter and Huntington, R.L., "Co-current Two-phase upward Flow of air and water through an open vertical Tube and through an annulus", Canadian Jr. of Chemical Engineering, 3, pp 248 (1961).

28. Alves, George, E., "Co-current Liquid Gas Flow in a Pipe line Contactor", Chemical Engineering Progress, Vol. 50, No. 9, pp. 449 (1954).

29. Wallis, G.B. "One dimensional Two-phase Flow", McGraw-Hill, New York (1969).

30. Tong, L.S., "Boiling Heat Transfer and Two-phase Flow", John Wiley and Sons, Inc., New York.

31. Sprenkle, R.E., "Piping Arrangement for Acceptable Flow meter Accuracy", Trans. ASME 67, pp. 345-360(1945)

32. Stearns, R.E. et al, "Flow Measurement with Orfice meters", D. Van Nostrand Comp. INC, Princeton New Jersey, pp 257, 311 and 246.

33. Flow Measurement, ASME POWER TEST Code; Supplement on Instruments and Apparatus, Part 5, Chapt. 4.

34. Marchaterre, John, F. and Barton M. Hoglud, "Correlation for Two-phase Flow", Nucleonics Vol. 20, pp 142 (August 1962).

35. Al-Seikh, J.N. et al, "Prediction of Flow Pattern in Horizontal Two-phase Pipe flow", The Canadian Journal of Chemical Engg., No. 1, pp 21 (Feb. 1970).

36. Isbin, H.S. et al, "A Model for correlating Two-phase Steam-water Burnout Heat Transfer Fluxes", Trans. of ASME Jr. of Heat Transfer, Vol. 83C, pp. 149 (May 1961).

# APPENDIX

## Design and Fabrication of an Air-Orifice Meter

### 1. Orifice-meter Installations

In providing and setting up the equipment for flow metering purposes, the initial step is the selection of orifice size and manometer range to handle the expected flow rate. Once these decisions have been made, the next problems encountered comprise generally of location of a suitable position for the orifice plate in the process line and design and installation of the orifice plate. Consideration must also be given to the type of orifice flanges and pressure tap connections used and to the location of a thermowell for temperature measurements. However, when possible, the pressure should be high enough so that small changes in pressure drop across the orifice have an inappreciable effect on the expansion factor Y. Thermometerwell should be placed atleast 10 I.D. preceding orifice plate.

Effect of Gas law deviations on metering accuracy -

As both the temperature and pressure of a gas approach their critical values considerably a widening deviation from the perfect gas law is exhibited. In the region near and particularly just below the critical

point, $\mu$ values are more sensitive to changes in temperature and pressure and it becomes increasingly difficult to evaluate gas density. Thus it is usually desirable to avoid the metering of gases near their critical points.

Orificemeter Pipe -

After providing sufficient length[31] of the pipe upstream and down stream, the pipe was used whose interior is nearly cylindrical, smooth and free from blisters, scale and rust as far as possible.

Line Size -

An Orifice plate should not be installed in lines less than 2" diameter. If line size for metering is not possible to have 2" of diameter, less accurate readings are encountered.

Position of Line -

Although an orifice plate may be located in either horizontal or a vertical line, installation in horizontal line is preferable in most cases. For liquid metering, location of an orifice plate in a vertical line with downward flow is not advisable, since under some conditions the liquid may fall free and may not fill the line.

Required Length of Straight Pipe -

For maximum accuracy, the orifice plate should be preceded by a straight section of constant diameter pipe at least 50 D internal pipe diameter long and should be followed by a similar pipe section at least 10 diameters long.

For minimum length a chart has been developed from the piping standards presented by Sprenkle[31].

From this chart, in our case diameter ratio $D_2/D_1 = \beta_1 = 0.3$.

Therefore, downstream length = 3 I.D.

upstream length = 6 I.D.

It should be noted that the upstream and downstream dimension given in these figures are minimum values which should be increased where conditions permit.

Pressure Taps : In general three types of pressure taps connection are used :

(i) Flange Taps - Upstream tap exactly 1 inch from upstream face of the plate, 1 inch down stream tap from down stream face.

(ii) Vena Contracta Taps - Upstream one I.D. from upstream face of the plate and centre of the downstream tap from Fig. 42 of Ref. 47. In our case 0.44 I.D. from downstream face minimum and 1.14 I.D. maximum.

(iii) Pipe Taps - Upstream $2\frac{1}{2}$ nominal pipe diameter from upstream face of the plate and downstream 8 nominal pipe diameter from down stream face of the plate.

Plate thickness, $C_1$ -

A minimum plate thickness of 1/16" is desirable.

Leading Edge Thickness, $C_2$ -

According to Gas measurement Committee (32)

$C_2 < \frac{1}{30} D$ , D = I.D. of pipe

$C_2 < \frac{1}{8} d$ , d = Orifice dia.

$C_2 < \frac{1}{4} \frac{D-d}{2}$

The minimum of these three should be taken.

In our case

$C_2 = 1.4$ mm

$C_1 = 5$ mm

$\beta_1 = 0.3$

$d = 12.6$ mm

$D = 42$ mm

If $C_2 < C_1$, then 45° bevelling is done.

Tap Connection - Here vena contracta tap connection has been used. Upstream - 42 mm from upstream face of orifice. Downstream - 18.5 mm from downstream face of orifice.

2. Basic Relations for the Measurement with Orificemeter :

General equation for orifice flow is

$$\sqrt{U_2^2 - U_1^2} = C\sqrt{2\,g\,\Delta h} \qquad (1)$$

$U_1$ - average velocity in the pipe at the upstream pressure tap, ft/sec.

$U_2$ - average velocity through the orifice at flow conditions

$\Delta h$- differential pressure across the orifice

C - coefficient of discharge

We know

$$U_1 A_1 = U_2 A_2$$

$$U_1 = U_2 \frac{A_2}{A_1} = U_2 \left(\frac{D_2}{D_1}\right)^2 = U_2\,\beta_1^2 \qquad (2)$$

Substituting this expression in (1), and simplifying,

$$U_2 = \frac{C\sqrt{2g\,\Delta h}}{\sqrt{1 - \beta_1^4}} \qquad (3)$$

$A_1$ = inside pipe cross-section. Area at the upstream pressure tap, sq.ft.

$A_2$ = Orifice area at flow temp., sq. ft.

$D_1$ = inside pipe diameter at upstream pressure tap

$D_2$ = orifice tap diameter at 60°F in.= d

$\beta_1 = D_2/D_1$

$\frac{1}{\sqrt{1 - \beta_1^4}}$ = velocity of approach factor

$$U_2 = K \sqrt{2 g \Delta h}$$

where $K = C/\sqrt{1-\beta_1^4}$ = orifice discharge coefficient.

In terms of mass rate

$$w = 3600 \rho_2 U_2 A_2 \quad (5)$$

$$A_2 = \alpha \frac{\pi}{4} (D_2/12)^2 \quad (6)$$

$\rho_2$ = density of fluid flowing through the orifice

$\alpha$ = An area multiplier which allows for thermal expansion or contraction of the orifice plate.

$$W = 157.5 (D_2)^2 \alpha K \rho_2 \sqrt{\Delta h} \quad (7)$$

The differential pressure in terms of inches of water

$$\Delta h = \frac{h_w}{12} \left[ \frac{62.37}{\rho_1} \right] \quad (8)$$

where $h_w$ = differential pressure across the orifice, inches of water at 60°F.

$\rho_1$ = density of fluid flowing at upstream pressure tap conditions, lb/cu.ft.

(7) becomes

$$w = 359.1 (D_2)^2 \alpha K \rho_2 \sqrt{\frac{h_w}{\rho_1}} \quad (9)$$

For compressible fluids, a change in density occurs as the fluid flows through the orifice from the upstream to the downstream section of the pipe. A dimensionless term, the expansion factor Y, is introduced to compensate for this density change.

Y = 1, in case of liquids,

therefore, $\rho_2 = Y_1 \rho_1$ (10)

Substituting (10) into (9)

$$w = 359.1 (D_2)^2 \alpha K Y_1 \sqrt{\rho_1 h_w} \quad (11)$$

For gas flow

$$\rho_1 = \frac{M P_1}{10.73 T_1 \mu_1} \quad (12)$$

This expression is based on perfect gas law allowing for deviations due to compressibility,

M – molecular weight of the gas

$P_1$ -absolute static pressure at the upstream pressure tap psia

$T_1$ -absolute temp. of the flowing fluid upstream side of the orifice

$\mu_1$ =gas law deviation (compressibility) factor at $P_1$ and $T_1$

10.73 = perfect law gas constant

3. Selection of orifice size and Manometer range –

The design of an orifice meter installation involves the choice of a suitable orifice diameter and manometer range.

Limits of $\beta_1$:

In flange taps, $\beta_1$ should be between 0.15 to 0.70 when Re $>$ 10,000; between 0.2 to 0.5 if it is not possible

to design with Re > 10,000.

In case of Vena contracta taps $\beta_1$ should be between 0.15 to 0.75 when Re > 10,000 between 0.2 to 0.5 if Re < 10,000.

In case of pipe taps, $\beta_1$ should be between 0.2 to 0.67 when Re > 10,000. For Re < 10,000, pipe taps should be avoided because of lack of data.

Calculation of $\beta_1$

$$w = 359.1 (D_2)^2 \alpha KY_1 \sqrt{\rho_1 h_w}$$

$$\rho_1 = \frac{M P_1}{10.73 T_1 \mu_1}$$

Maximum discharge expected = 91.7 lbs/hr.

$$91.7 = \frac{359.1}{\sqrt{10.73}} \beta_1^2 D_1^2 \alpha KY_1 \sqrt{\frac{h_w M P_1}{T_1 \mu_1}}$$

$$91.7 = \frac{359.1}{\sqrt{10.73}} \beta_1^2 x (1.65)^2 x\ 1\ x\ K\ x\ 1 \sqrt{\frac{h_w M P_1}{T_1 x\ 1}}$$

M = 28.96

P = 39.7 psia

T = 68°F

$h_w$ = 24"

Substituting values, we get

$\beta_1^2$ = 0.267

is chosen as 0.3

Orifice diameter = 42x0.3 = 12.6 mm.

$C_2$ = 1.4 mm

$C_1$ = 5 mm.

4. Calculation of Meter Factor and Flow Rate

$$w = 359.1\ (D_2)^2 \alpha K \sqrt{\rho_1 h_w} \quad \text{lbs/hr.}$$

$$= \frac{359.1}{\sqrt{10.79}} \beta_1^2 D_1^2 \alpha K Y_1 \sqrt{\frac{h_w M P_1}{T_1 \mu_1}}$$

$$= \frac{359.1 \times 0.3^2 \times 1.65^2}{\sqrt{10.73}} \alpha K Y_1 \sqrt{\frac{h_w M P_1}{T_1 \mu_1}}$$

$$= 26.85\ K Y_1 \sqrt{\frac{h_w M P_1}{T_1 \mu_1}}$$

For air M = 28.96

$$w = 144\ K Y_1 \alpha \sqrt{\frac{h_w P_1}{T_1 \mu_1}} \quad \text{lbs/hr}$$

$\alpha$ = 1 from 50°F to 90°F (Ref.47)

Gas law deviation (compressibility factor)

$\mu_1 = \frac{P_1 V_1}{RT_1} \simeq 1$ for pressure 0 to 30 psi a plot of $\mu_1$ vs. pressure, temperature as parameter is given[32].

A plot of $Y_1$ vs. $\frac{\Delta p}{KP_1}$ is given with $\beta_1$ as parameter[32].

$\Delta P$ = differential pressure

$K = \frac{C_p}{C_v}$ = 1.4 for air

$Y_1$ = 1 for the compressor and manometer used.

Finally

$$w = 144\ K\sqrt{\frac{h_w P_1}{T_1}} \quad \text{lbs/hr.}$$

$P_1$ is inlet pressure in psia,

and $T_1$ is the inlet temperature.

A table for K as a function of Reynold's number is given[33].

Procedure to calculate flow rates :

(i) For a particular value of K from the table, w is calculated

(ii) Inlet velocity is calculated.

(iii) Reynold's number is calculated.

(iv) For the calculated Reynold's number, value of K is taken from the table and corresponding w calculated.

(v) Again with this flow rate, Reynold's number is calculated and value of K taken, which is final for calculating w

Value of K for 1.625" I.D. i.e. 42 mm I.D. and Vena contracta pressure taps and $\beta_1 = 0.3$.

| $R_D$ | 500 | 1000 | 2000 | 3000 | 4000 | 5000 | 6000 | |
|---|---|---|---|---|---|---|---|---|
| K | 0.6505 | 0.6276 | 0.6186 | 0.6145 | 0.6121 | 0.6105 | 0.6093 | |
| $R_D$ | 8000 | 10,000 | 15,000 | 20,000 | 25,000 | 50,000 | $10^5$ | $10^6$ |
| K | 0.6076 | 0.6064 | 0.6045 | 0.6036 | 0.6028 | 0.6010 | 0.5997 | 0.5976 |

TABLE No. 1

Pressure drop in two phase air water flow at 1.1736kgf/cm$^2$abs. inlet pressure.

| Air-flow $Kg_m/hr$ | Water-flow $Kg_m/hr$ | Inlet pressure kgf/cm$^2$ abs. | $(\frac{\Delta P}{\Delta Z})_{TPF}$ X0.012 mm of water per mtr | G X 0.205 X$10^{-4}$ Kgm/hr.m$^2$ | x% Air weight fraction | Superficial air-velocity $V_{gs}$ m/sec | Gms of water/mtr$^3$ of air | $\frac{G_g}{10^4}$ | $(\frac{G_l}{G_g})\lambda$ $10^{-2}$ |
|---|---|---|---|---|---|---|---|---|---|
| 19.6 | 0.9 | 1.1736 | 1.21 | 4.052 | 95.6 | 37.65 | 63.8 | 3.6 | 4.92 |
| 17.35 | 0.9 | 1.1736 | 1.125 | 3.597 | 95.2 | 33.4 | 72 | 3.18 | 5.57 |
| 14.8 | 0.932 | 1.1736 | 1.0 | 3.094 | 94 | 28.55 | 87.5 | 2.71 | 6.8 |
| 11.78 | 1.08 | 1.1736 | 0.875 | 2.5323 | 91.8 | 22.65 | 127.5 | 2.16 | 9.85 |

TABLE No.3

Pressure Drop in Two-phase Air-water flow at 1.5954 kgf/cm$^2$ abs. inlet pressure

| Air-flow $Kg_m/hr.$ | Water-flow $Kg_m/hr$ | Inlet pressure Kgf/cm$^2$ abs. | $(\frac{\Delta P}{\Delta Z})_{TPF}$ x0.012 mm of water per mtr | G x 0.205 x $10^{-4}$ Kgm/hr. $m^2$ | x% Air weight fraction | Superficial Air velocity $V_{gs}$ m/sec | Gms.of water $mtr^3$ of air | $(\frac{G_g}{\lambda})$ $10^4$ | $(\frac{G_l}{G_g})\lambda\psi$ $10^{-2}$ |
|---|---|---|---|---|---|---|---|---|---|
| 40.3 | 1.44 | 1.5954 | 3.185 | 8.23 | 96.5 | 56.8 | 67.6 | 6.35 | 4.48 |
| 36.8 | 1.392 | 1.5954 | 3.0 | 7.5242 | 96.3 | 52 | 71.6 | 5.78 | 4.75 |
| 32.8 | 1.35 | 1.5954 | 2.9 | 6.726 | 96.2 | 46.3 | 77.8 | 5.17 | 4.95 |
| 28.4 | 1.35 | 1.5954 | 2.75 | 5.856 | 95.5 | 40 | 90 | 4.47 | 5.75 |
| 23.1 | 1.232 | 1.5954 | 2.5 | 4.7925 | 94.8 | 32.6 | 101 | 3.63 | 6.68 |
| 20.75 | 1.35 | 1.5954 | 2.34 | 4.328 | 94 | 29.2 | 123 | 3.26 | 7.6 |

TABLE NO.4

Regimes Photographed at different air flow and water flow rates.

| S.No | Airflow rate kg/hr | Water flow rate kg/hr | Air superficial velocity $V_{gs}$ m/sec | Water Superficial velocity $V_{fs}$ mm/sec | Fig. No. |
|---|---|---|---|---|---|
| 1 | 27.8 | 0.3 | 47.8 | 0.8 | 13(a) |
| 2 | 27.8 | 0.39 | 47.8 | 1.04 | 13(b) |
| 3 | 27.8 | 0.42 | 47.8 | 1.12 | 14(a) |
| 4 | 27.8 | 0.54 | 47.8 | 1.44 | 14(b) |
| 5 | 27.8 | 0.72 | 47.8 | 1.92 | 15(a) |
| 6 | 27.8 | 0.9 | 47.8 | 2.4 | 15(b) |
| 7 | 27.8 | 1.26 | 47.8 | 3.36 | 16(a) |
| 8 | 18.0 | 1.2 | 31 | 3.2 | 16(b) |
| 9 | 18.0 | 0.87 | 31 | 2.32 | 17(a) |
| 10 | 11.64 | 0.54 | 20.0 | 1.44 | 17(b) |
| 11 | 9.88 | 0.93 | 17 | 2.48 | 18(a) |
| 12 | 8.7 | 0.99 | 14.95 | 2.64 | 18(b) |

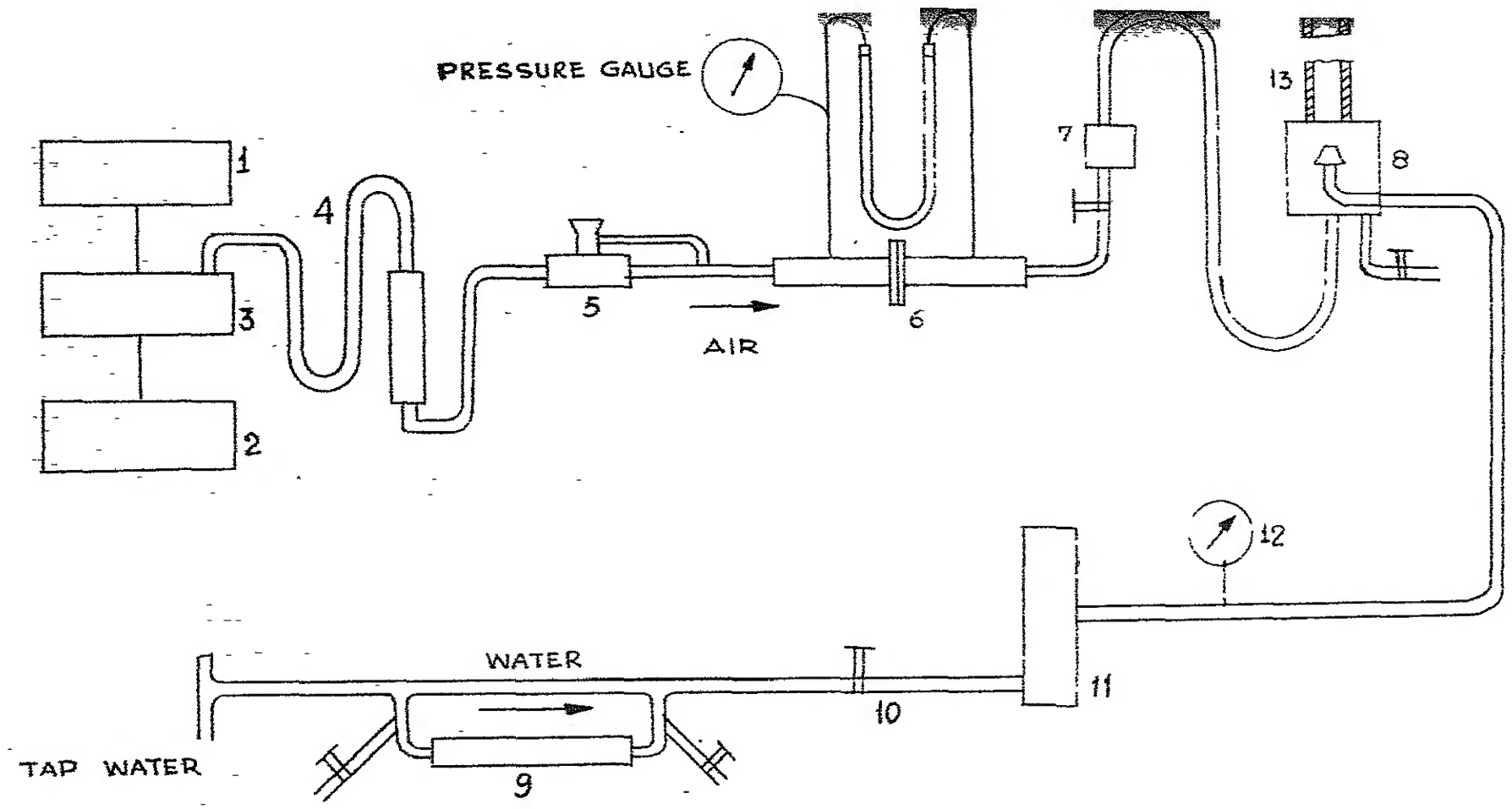


1,2,3 AIR COMPRESSORS
4 DEHUMIDIFIER
5 PRESSURE REDUCING VALVE
6 ORRIFICE METER
7 NONRETURN VALVE
8 MIXER
9 DYE CONTAINER
10 CONTROL VALVE
11 ROTA METER
12 WATER PRESSURE GAUGE
13 TEST SECTION

FIG. 1

Schematic Diagram of Experimental Equipment

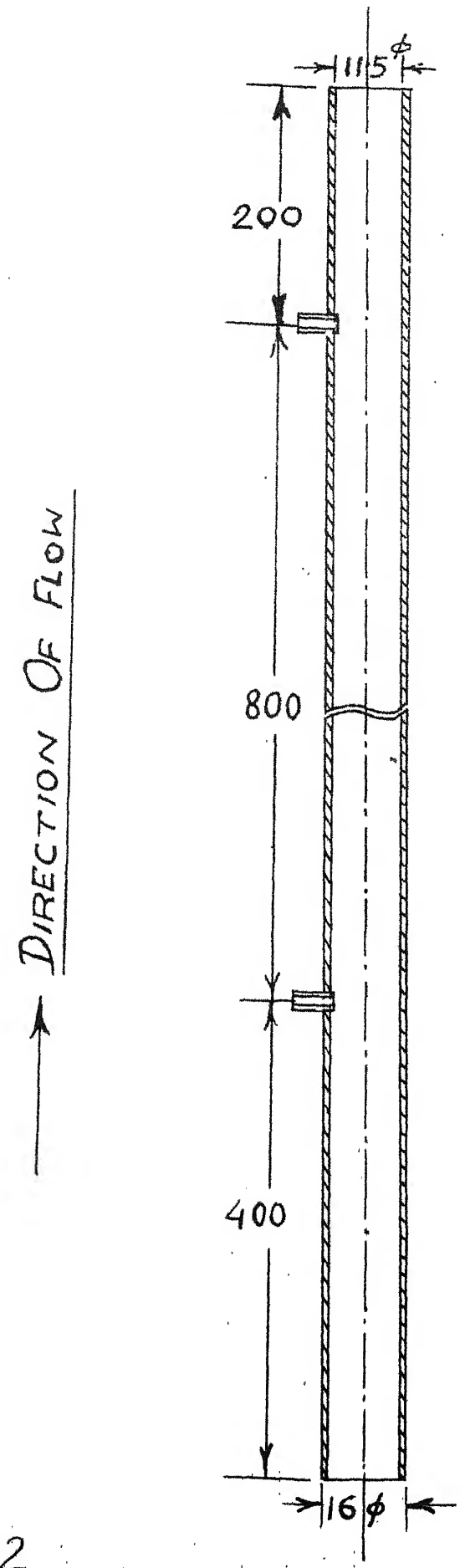


SECTIONAL ELEVATION
DIMENSIONS IN MM

TEST SECTION

FIG. 2

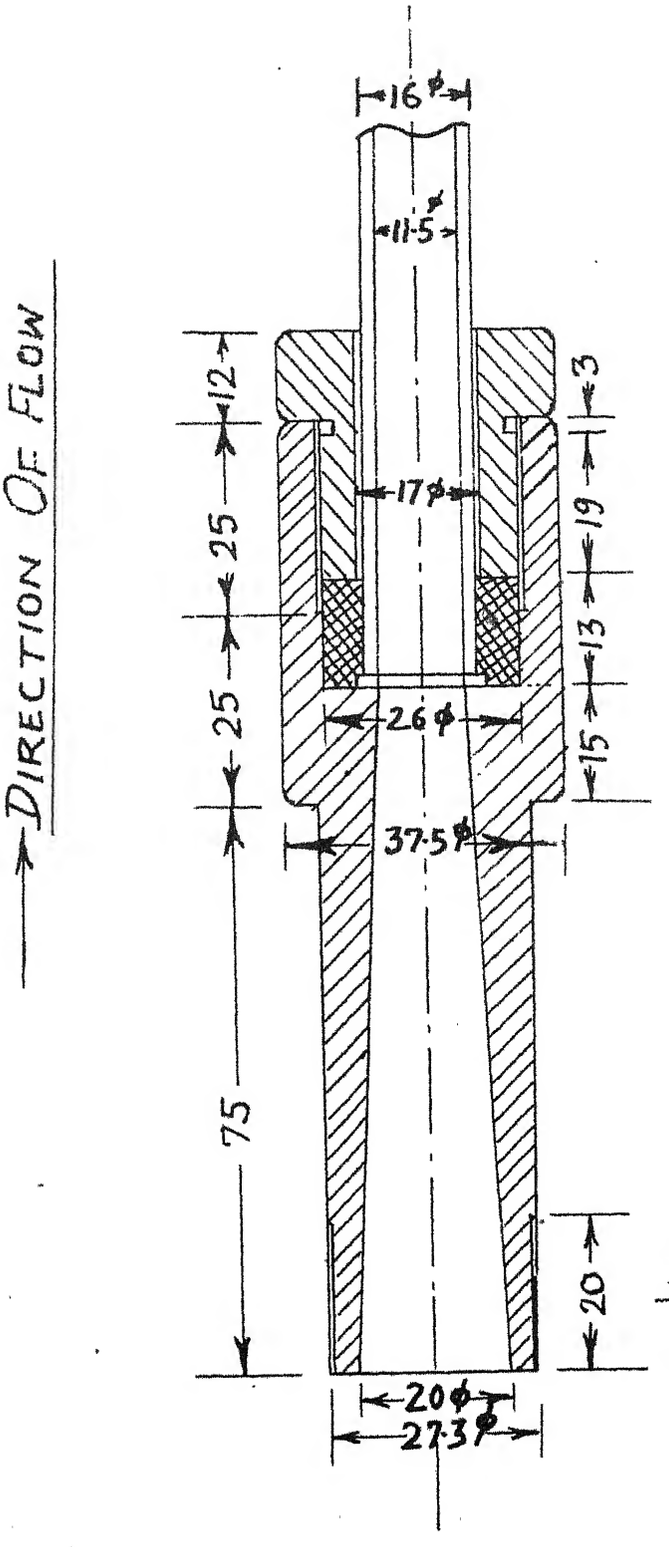


FIG 3

# TEST SECTION WITH END CONNECTION

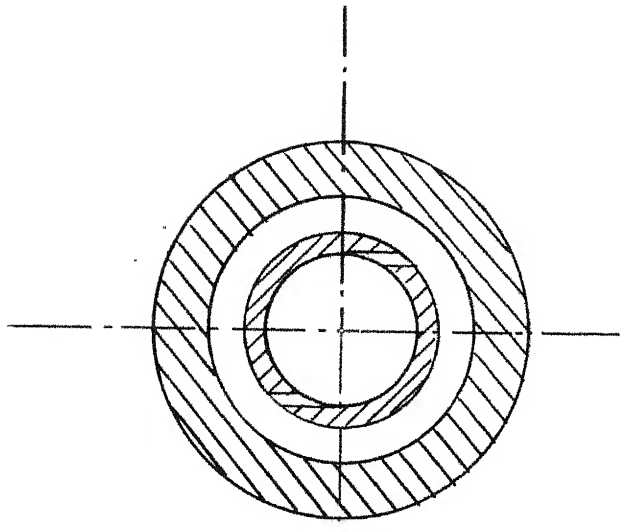

SECTION AT XX

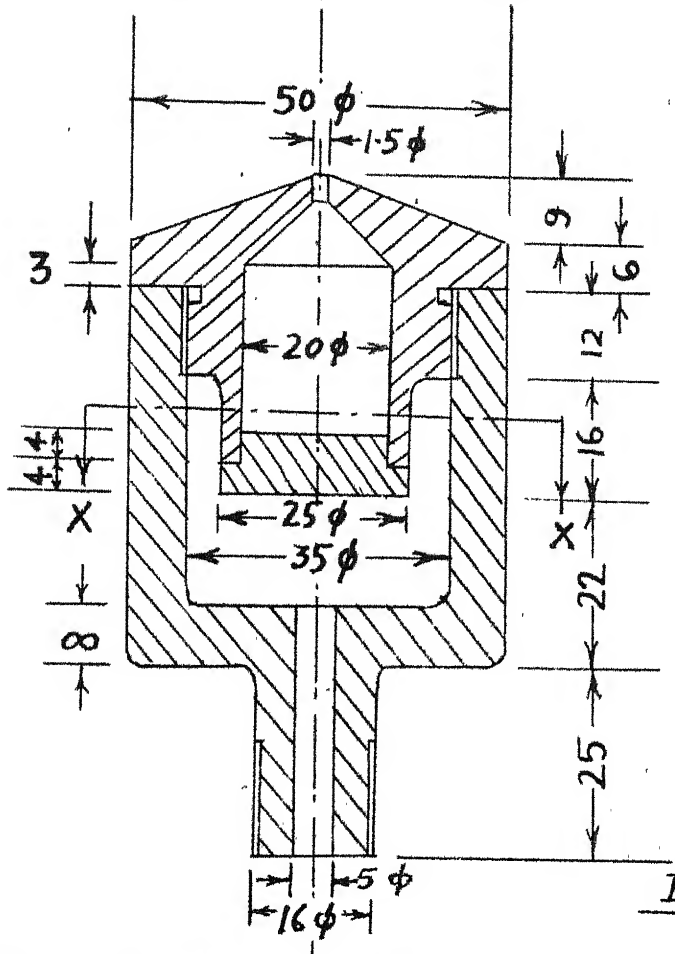


DIMENSIONS IN MM.

SECTIONAL ELEVATION

FIG 4

# WATER SPRAYER

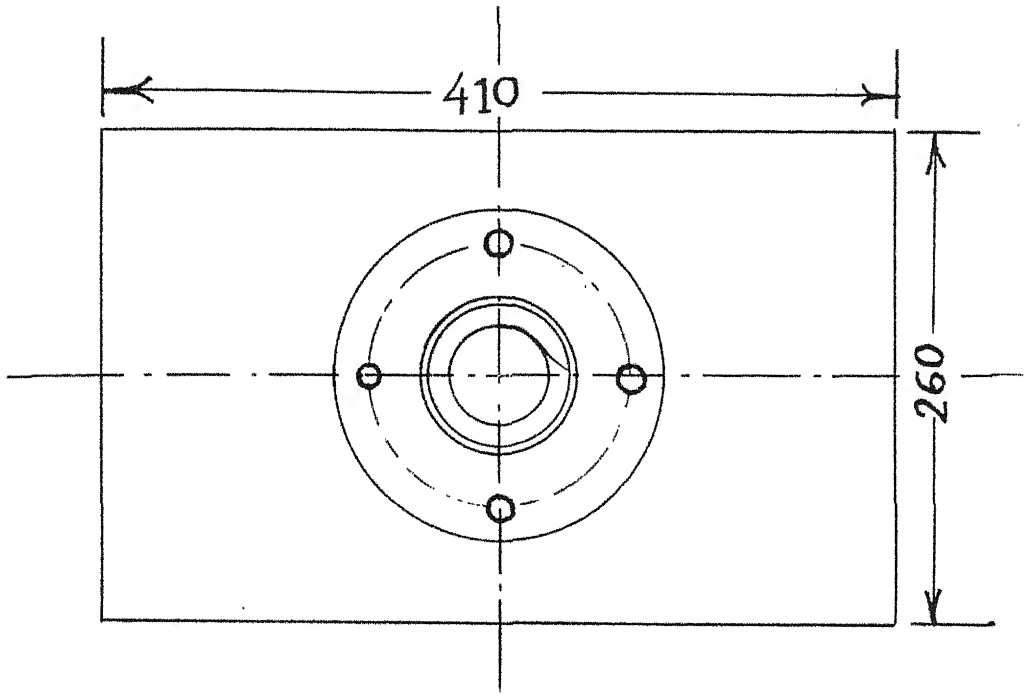


PLAN

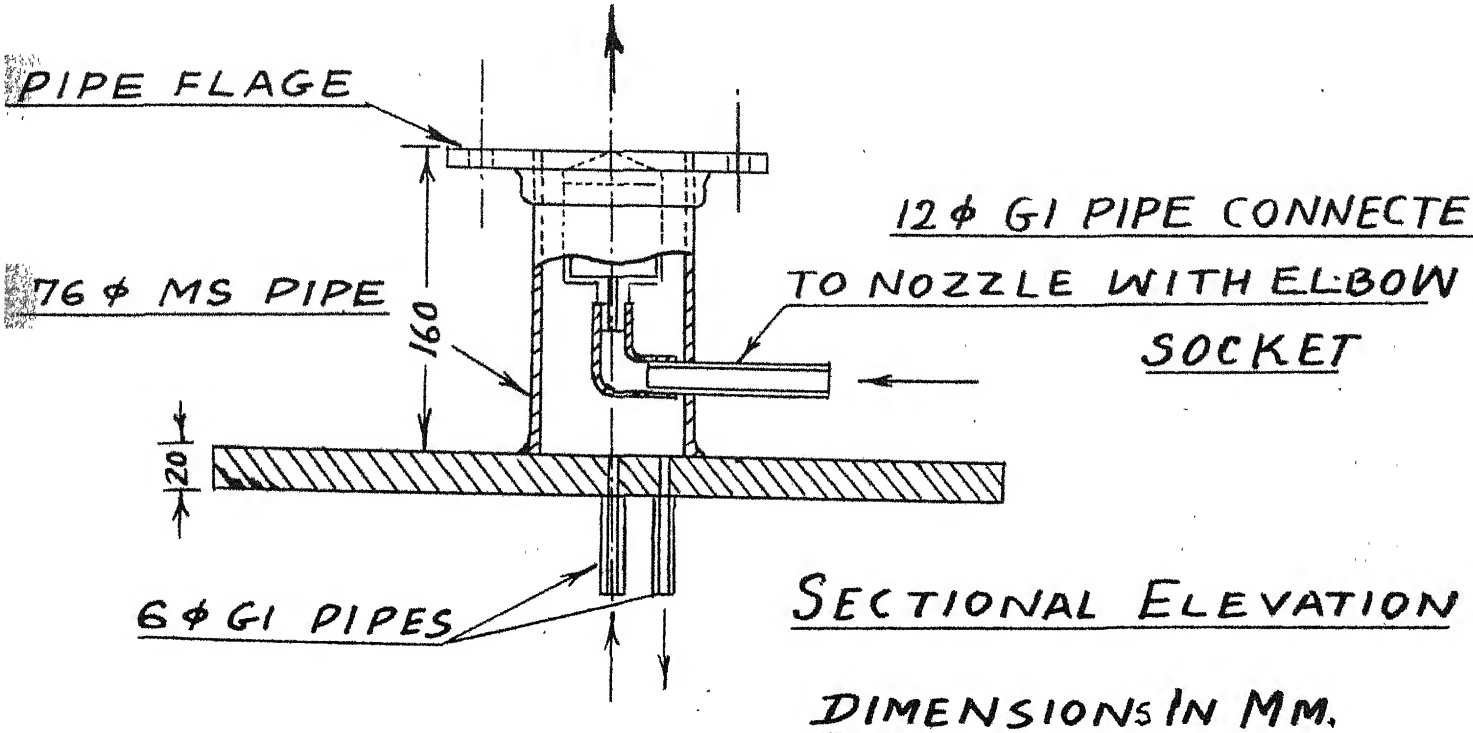


SECTIONAL ELEVATION

DIMENSIONS IN MM.

FIG 5

# MIXING CHAMBER

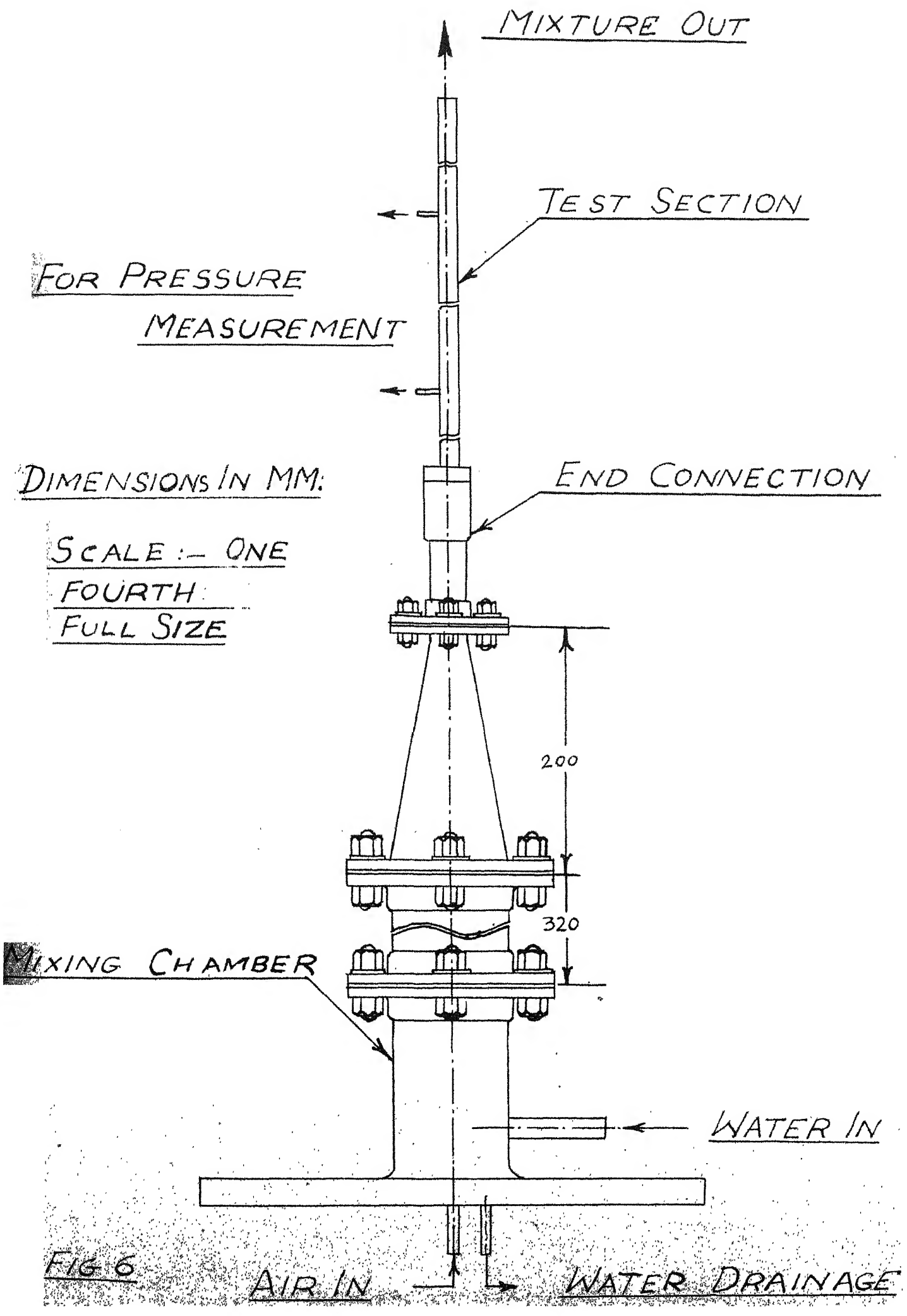
MIXTURE OUT
TEST SECTION
FOR PRESSURE MEASUREMENT
DIMENSIONS IN MM:
SCALE :- ONE FOURTH FULL SIZE
END CONNECTION
200
320
MIXING CHAMBER
WATER IN
AIR IN
WATER DRAINAGE

FIG 6

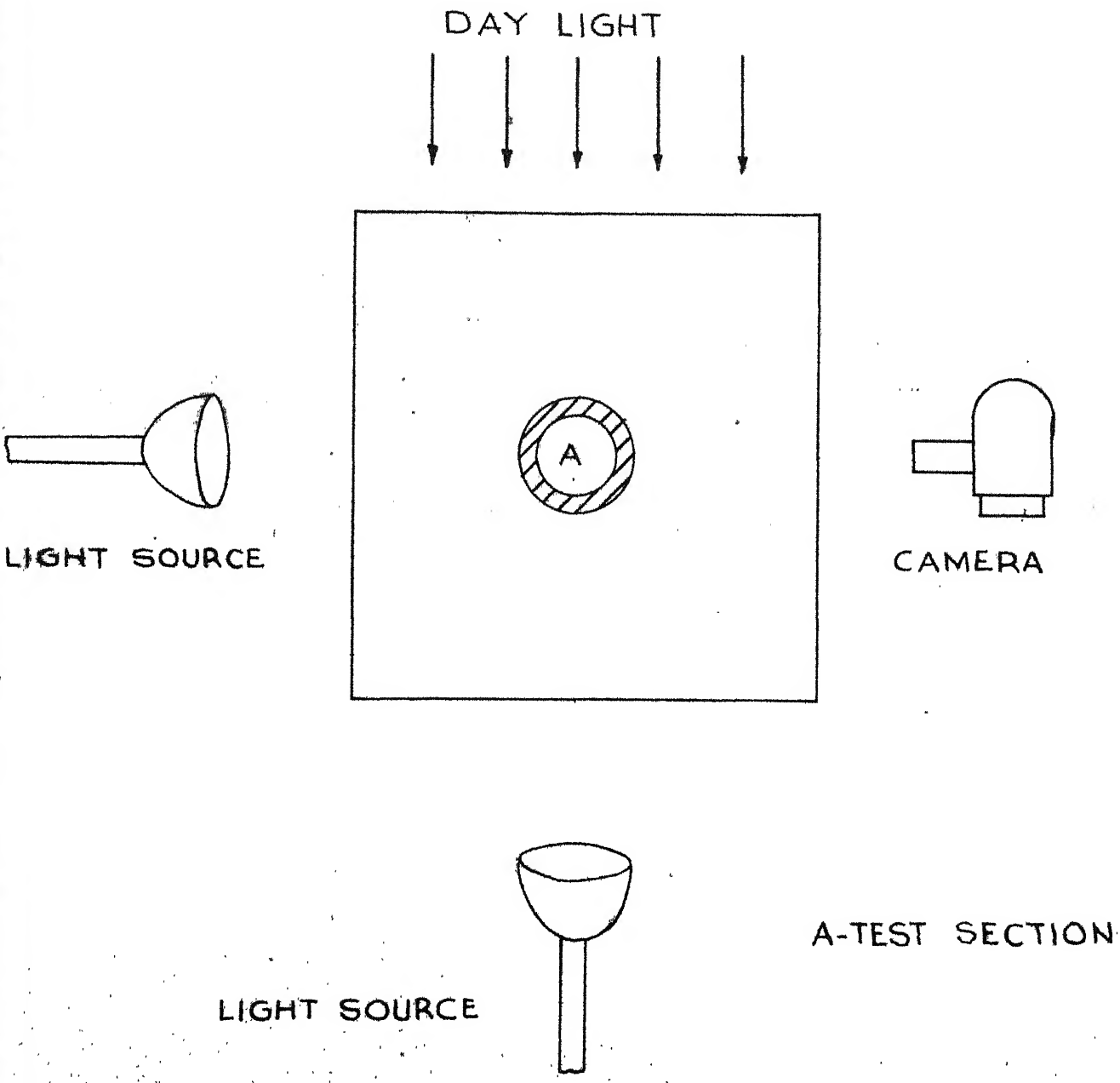


PHOTOGRAPHIC SETUP

FIG 6a

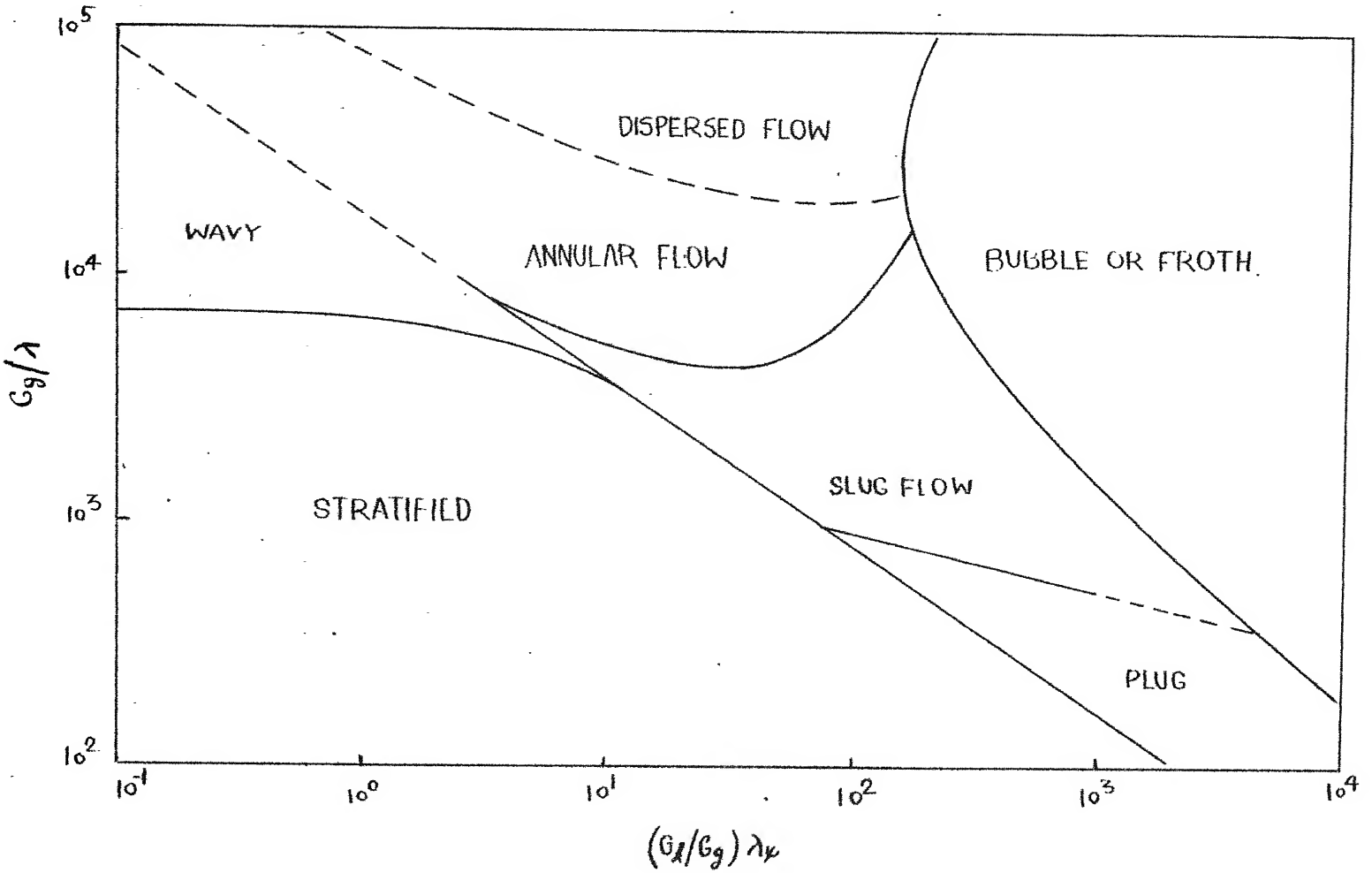


FLOW REGIMES AS DESIGNATED BY BAKER

FIG. 7

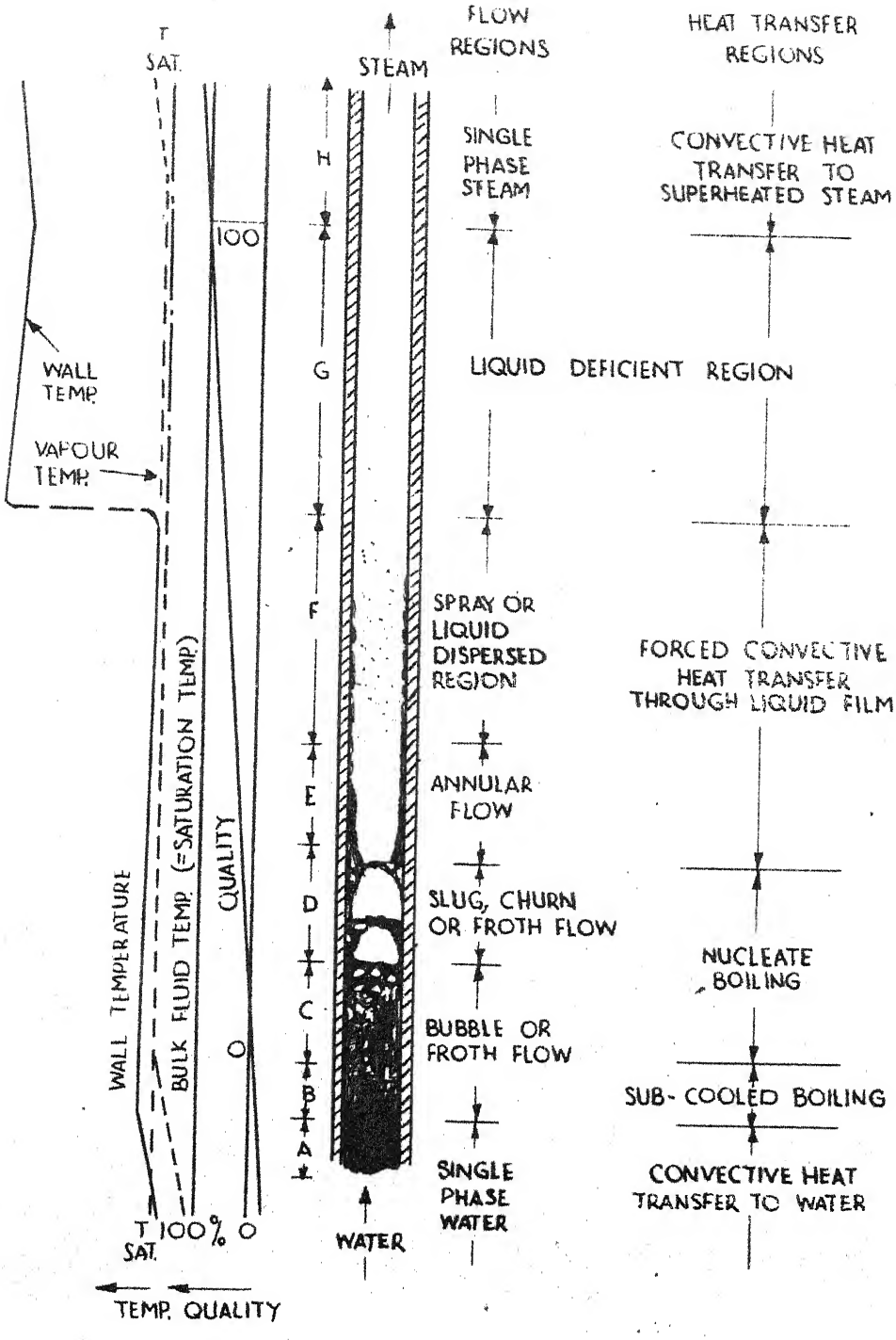


FIG. 8

REGIMES OF TWO-PHASE FLOW

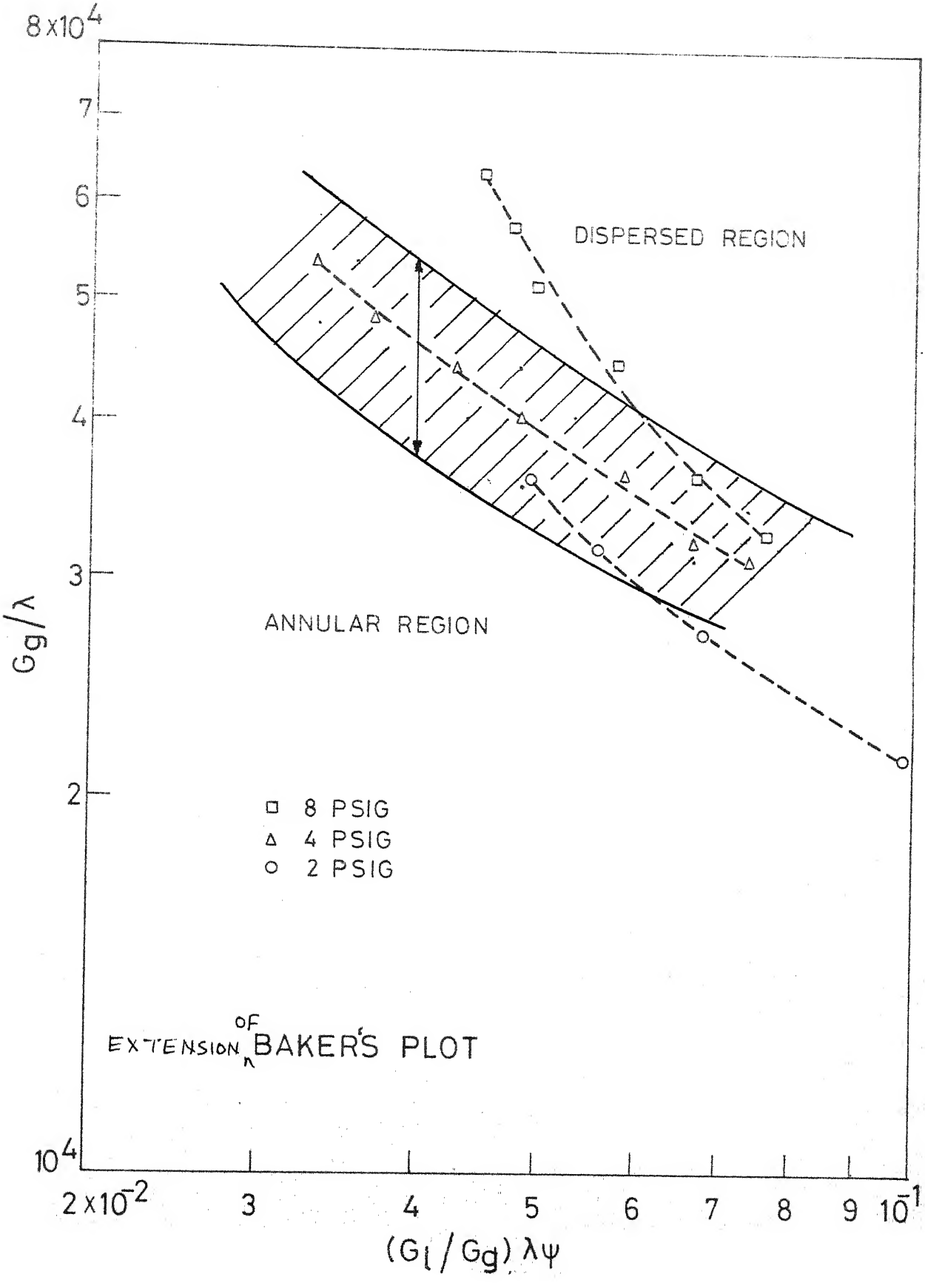
8x10^4
7
6
5
4
3
2
10^4
Gg/λ
DISPERSED REGION
ANNULAR REGION
8 PSIG
4 PSIG
2 PSIG
EXTENSION OF BAKER'S PLOT
2x10^-2
3
4
5
6
7
8
9
10^-1
(Gl/Gg) λψ

FIG. 9

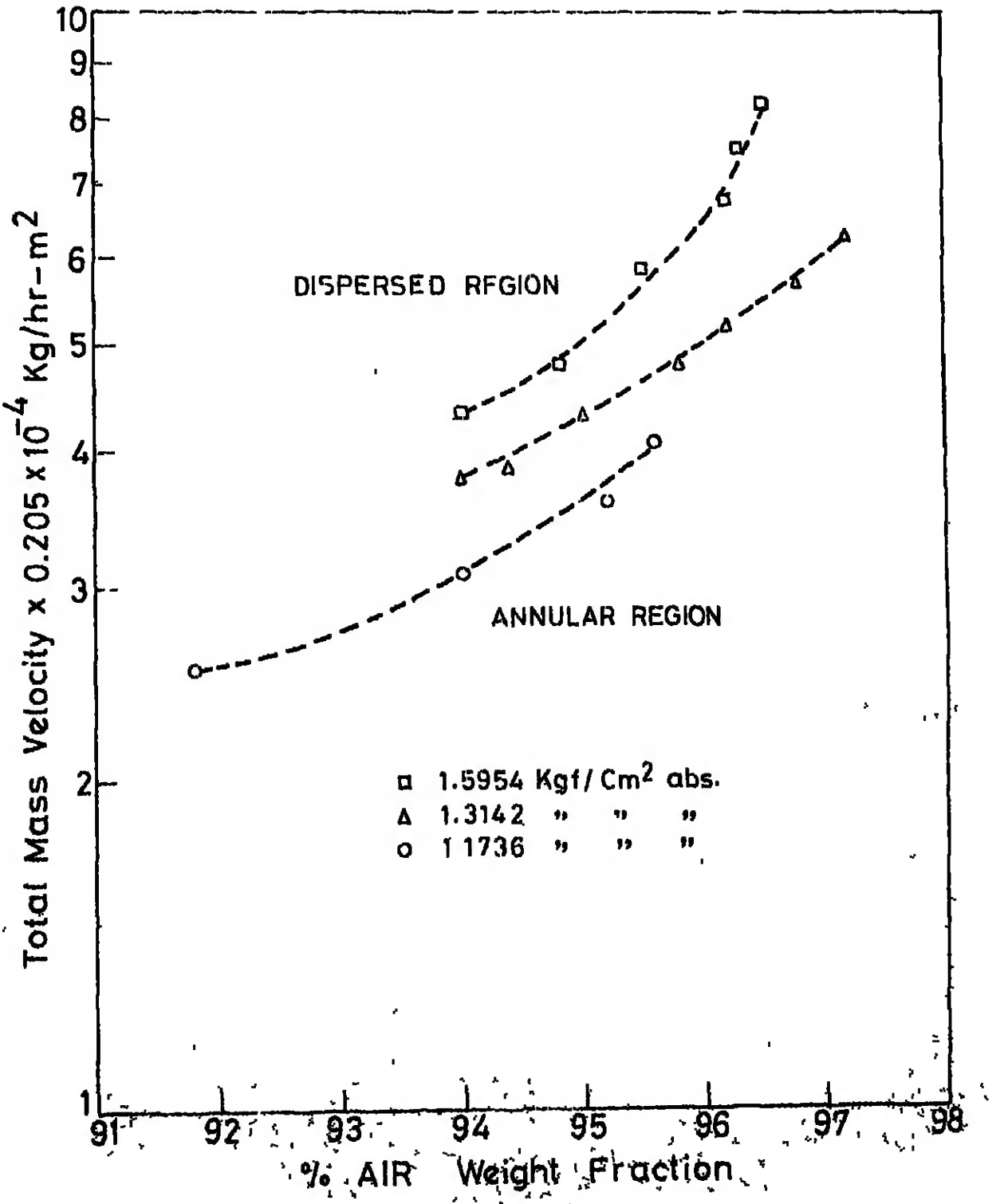
Total Mass Velocity x 0.205 x $10^{-4}$ Kg/hr-$m^2$
10
9
8
7
6
5
4
3
2
1
DISPERSED REGION
ANNULAR REGION
□ 1.5954 Kgf/ $Cm^2$ abs.
Δ 1.3142 " " "
o 1 1736 " " "
91
92
93
94
95
96
97
98
% AIR Weight Fraction

FIG. 10

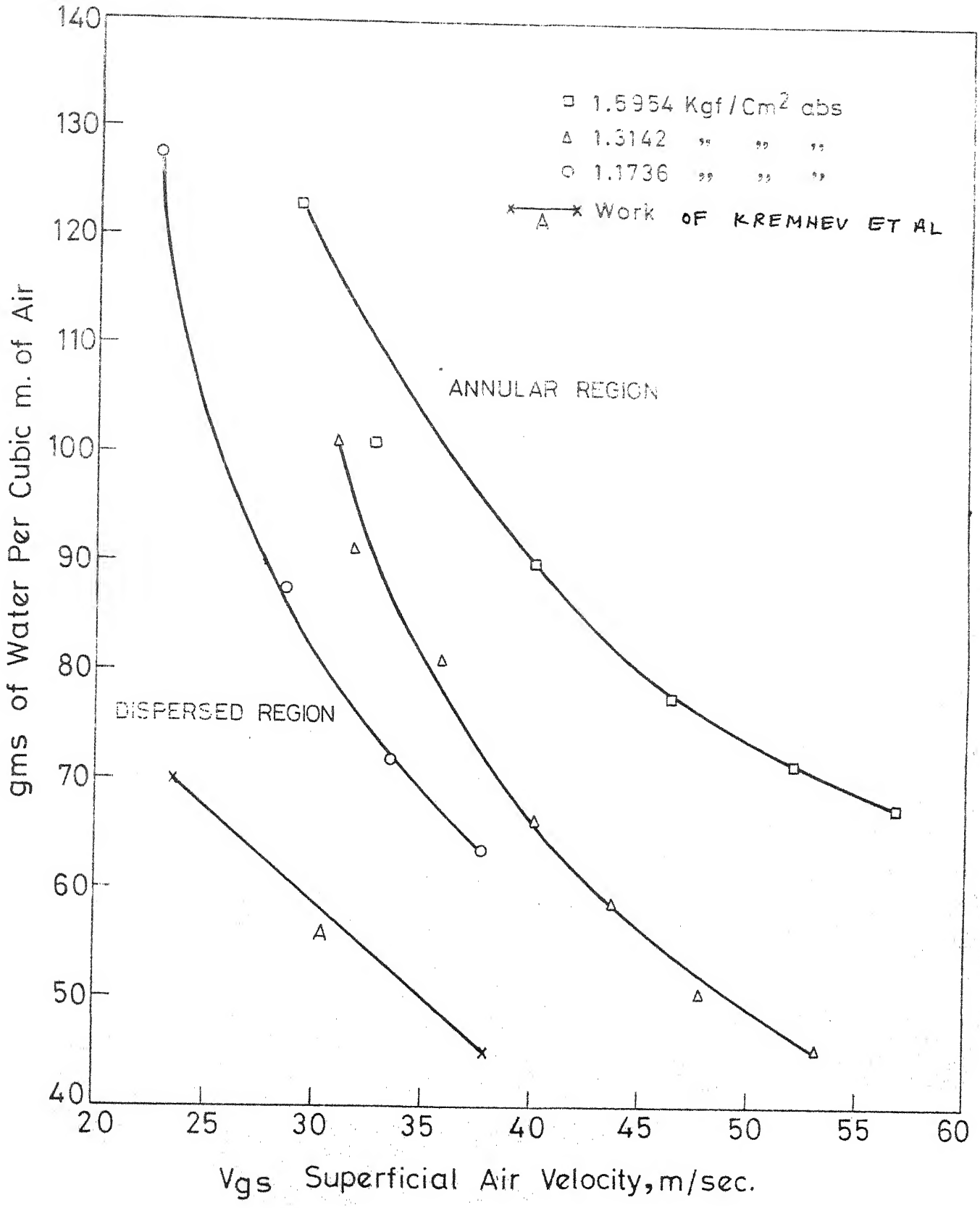
□ 1.5954 Kgf/Cm² abs
△ 1.3142 " " "
○ 1.1736 " " "
×—×A Work OF KREMNEV ET AL
ANNULAR REGION
DISPERSED REGION
A
gms of Water Per Cubic m. of Air
Vgs Superficial Air Velocity, m/sec.
140
130
120
110
100
90
80
70
60
50
40
20
25
30
35
40
45
50
55
60

FIG. 11

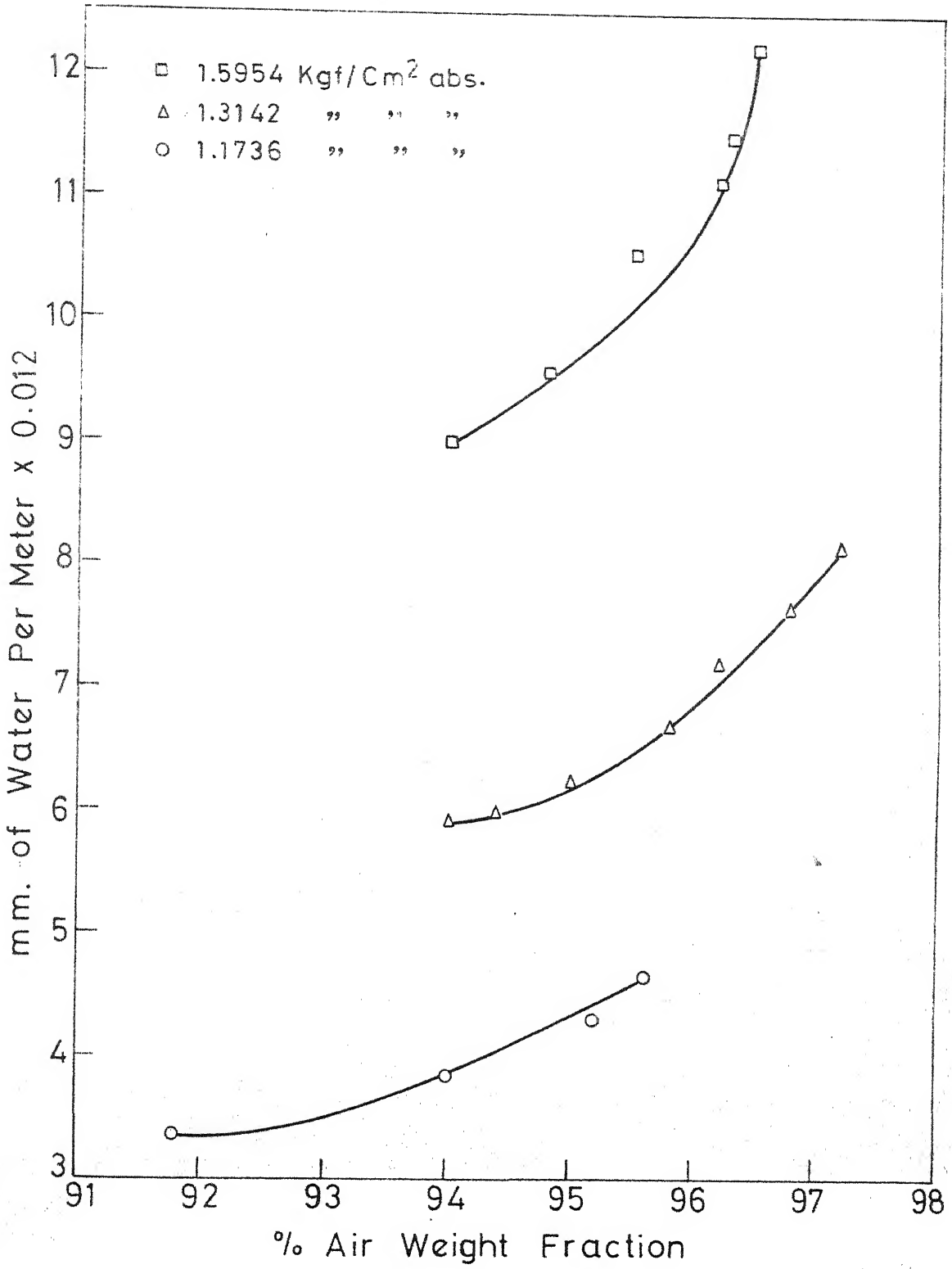
□ 1.5954 Kgf/Cm² abs.
△ 1.3142 " " "
○ 1.1736 " " "
mm. of Water Per Meter x 0.012
% Air Weight Fraction
12
11
10
9
8
7
6
5
4
3
91
92
93
94
95
96
97
98

FIG. 12

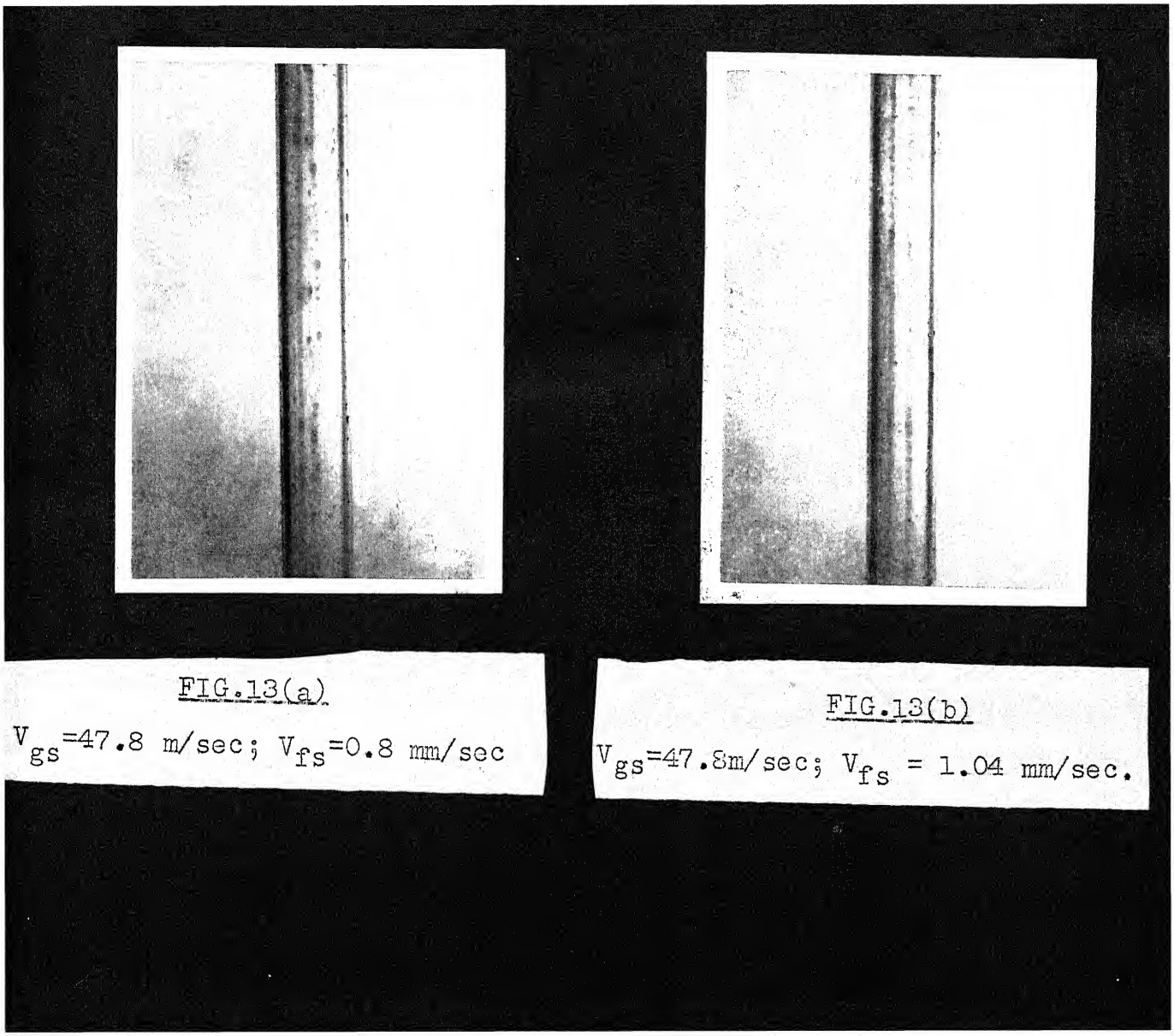

FIG.13(a)

$V_{gs}$=47.8 m/sec; $V_{fs}$=0.8 mm/sec

FIG.13(b)

$V_{gs}$=47.8m/sec; $V_{fs}$ = 1.04 mm/sec.

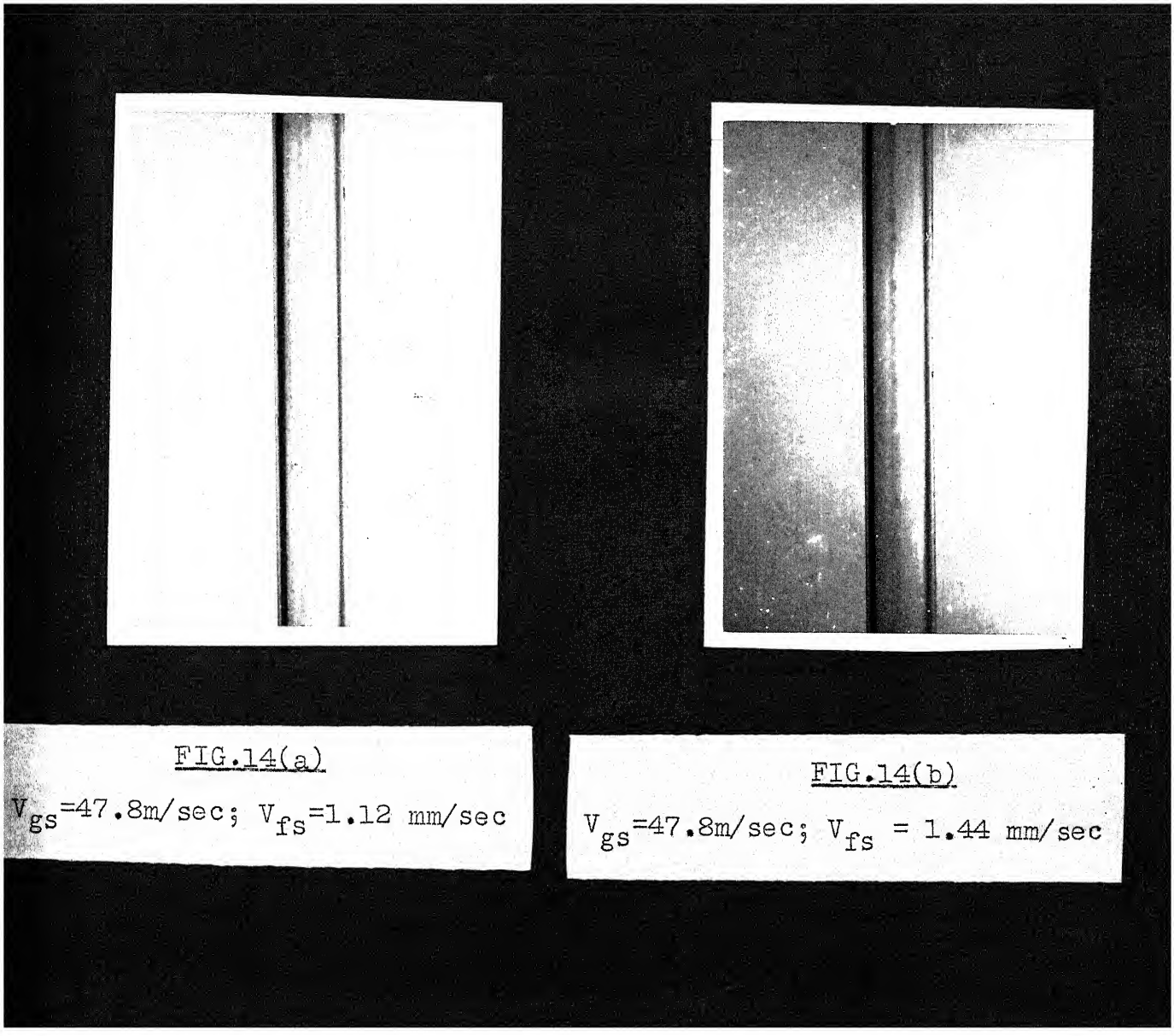

FIG.14(a)

$V_{gs}$=47.8m/sec; $V_{fs}$=1.12 mm/sec

FIG.14(b)

$V_{gs}$=47.8m/sec; $V_{fs}$ = 1.44 mm/sec

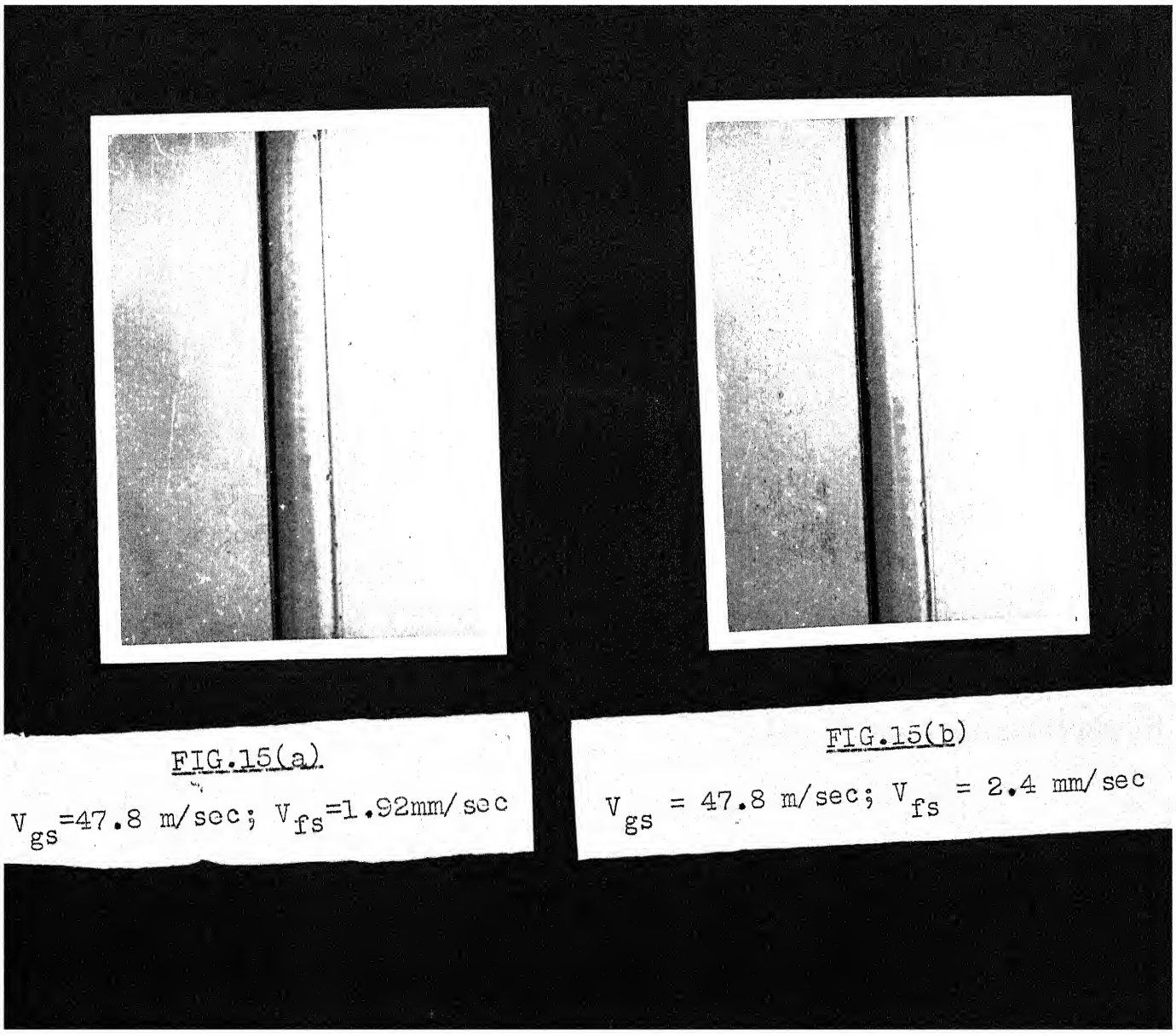

FIG.15(a)

$V_{gs}$=47.8 m/sec; $V_{fs}$=1.92mm/sec

FIG.15(b)

$V_{gs}$ = 47.8 m/sec; $V_{fs}$ = 2.4 mm/sec

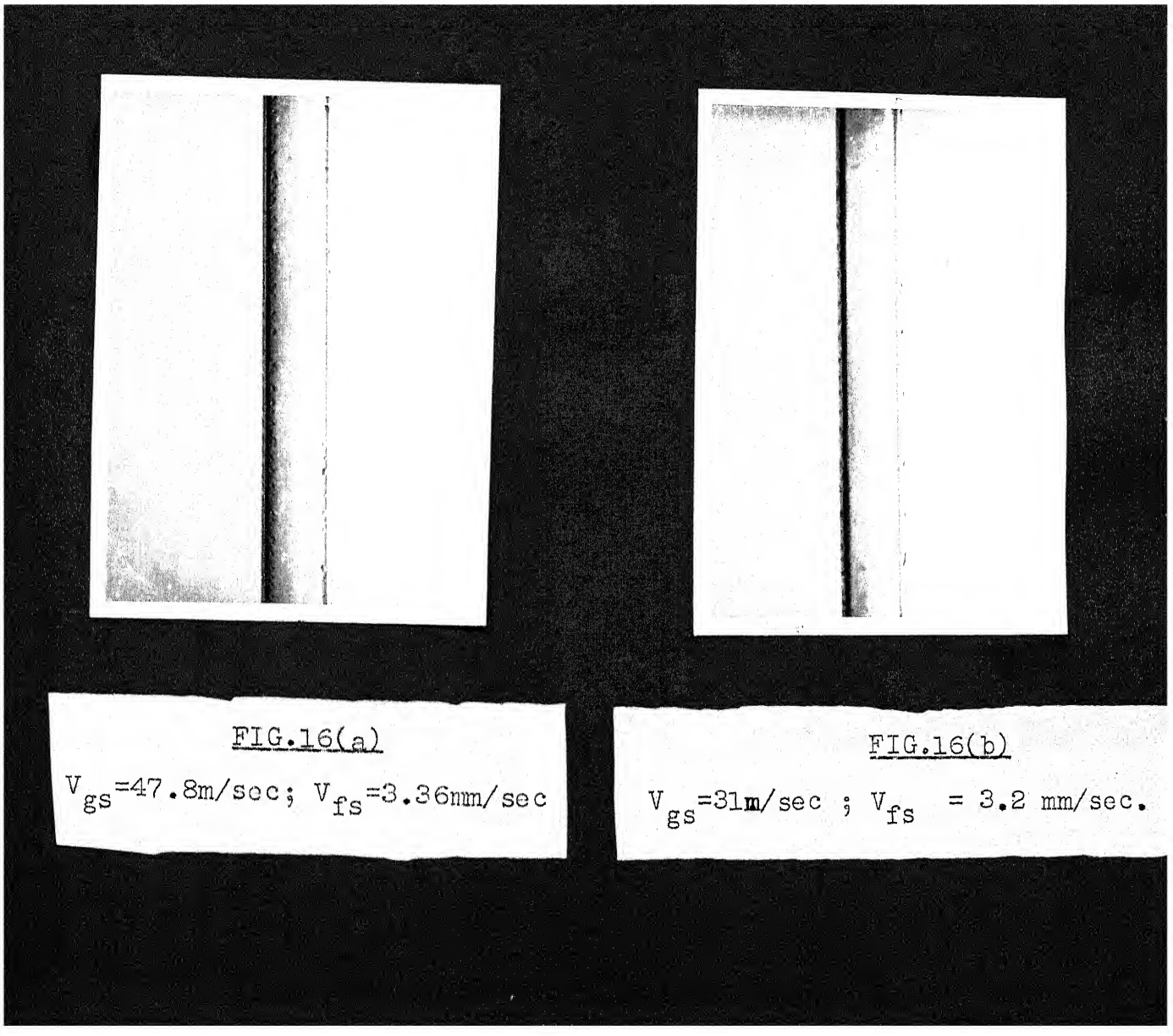

FIG.16(a)

$V_{gs}$=47.8m/sec; $V_{fs}$=3.36mm/sec

FIG.16(b)

$V_{gs}$=31m/sec ; $V_{fs}$ = 3.2 mm/sec.

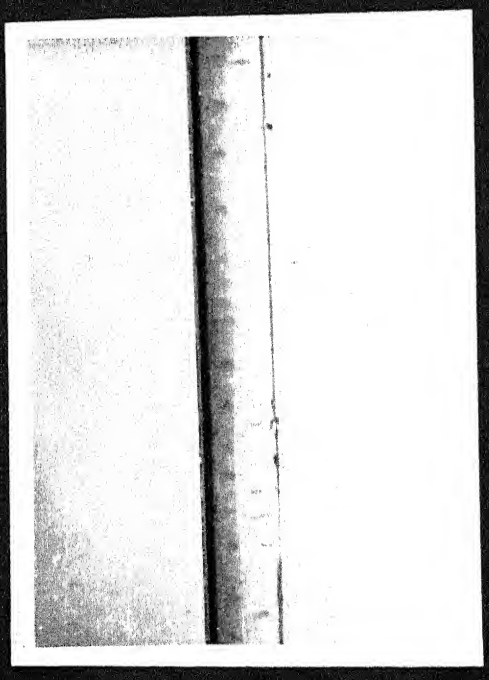

FIG.17(a)

$V_{gs}$= 31m/sec; $V_{fs}$=2.32 mm/sec

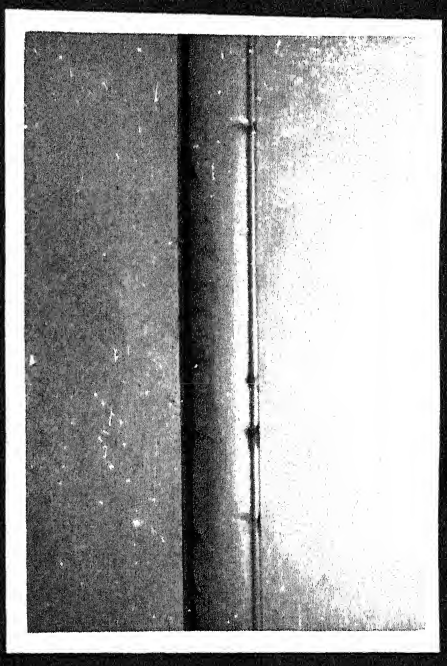

FIG.17(b)

$V_{gs}$ = 20 m/sec; $V_{fs}$ = 1.44 mm/sec.

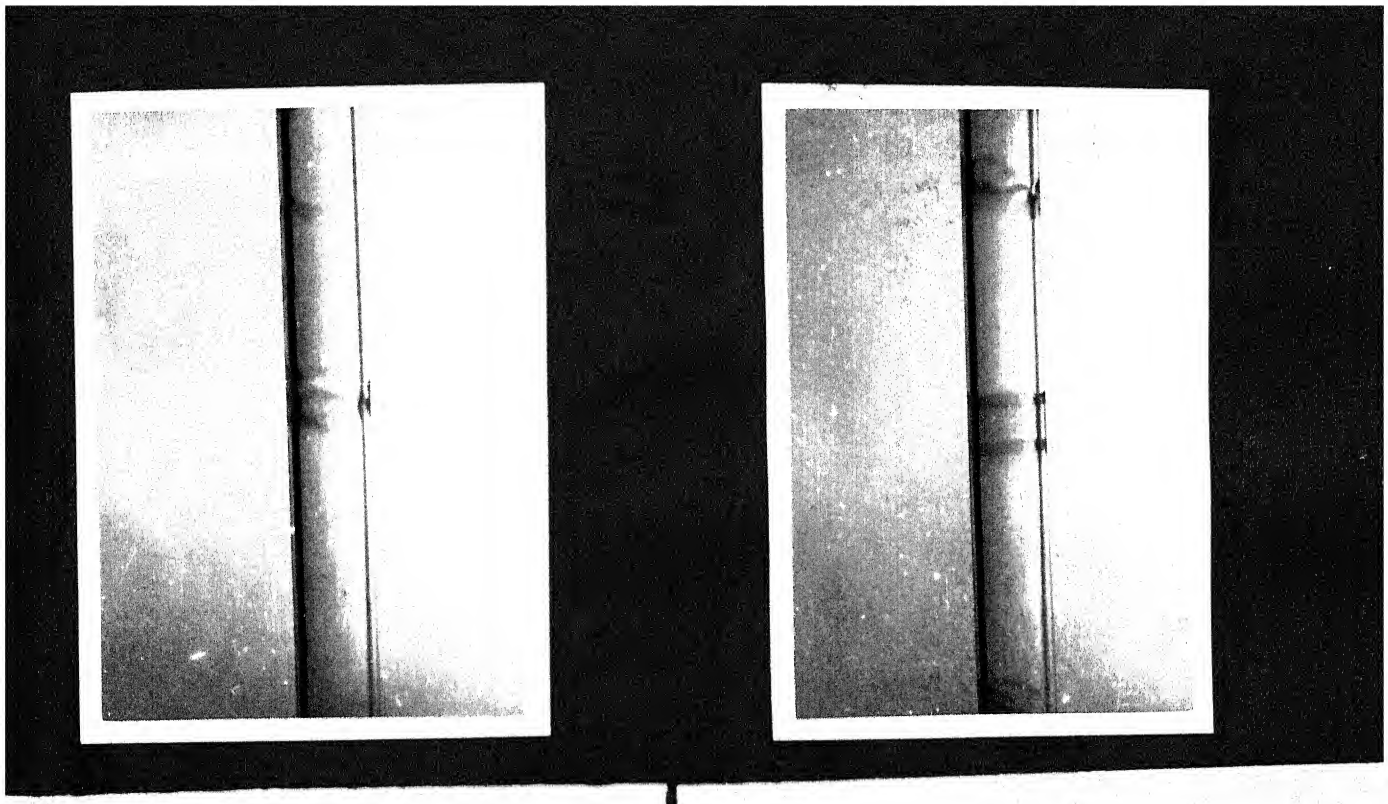

FIG.18(a)

$V_{gs}$= 17m/sec; $V_{fs}$ = 2.48mm/sec

FIG.18(b)

$V_{gs}$ = 14.95m/sec; $V_{fs}$ = 2.64 mm/sec.

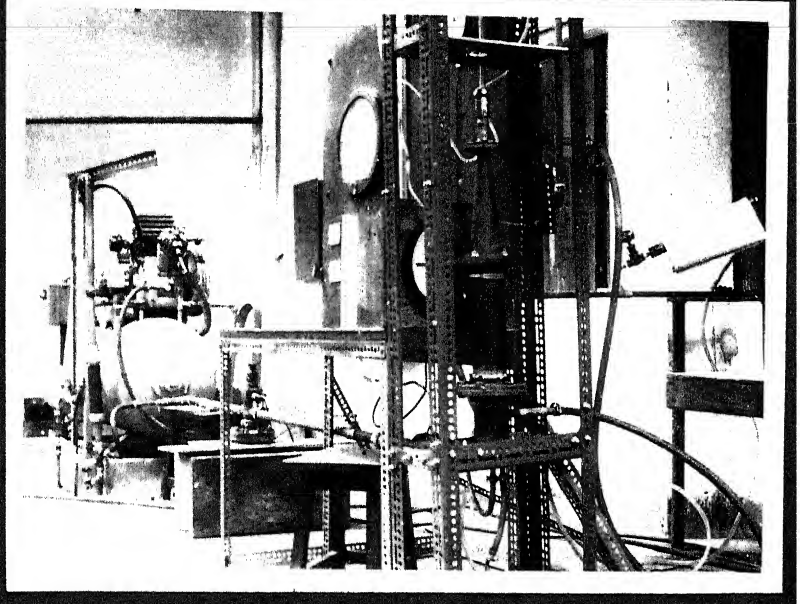

FIG.19

Full View of the Experimental set up

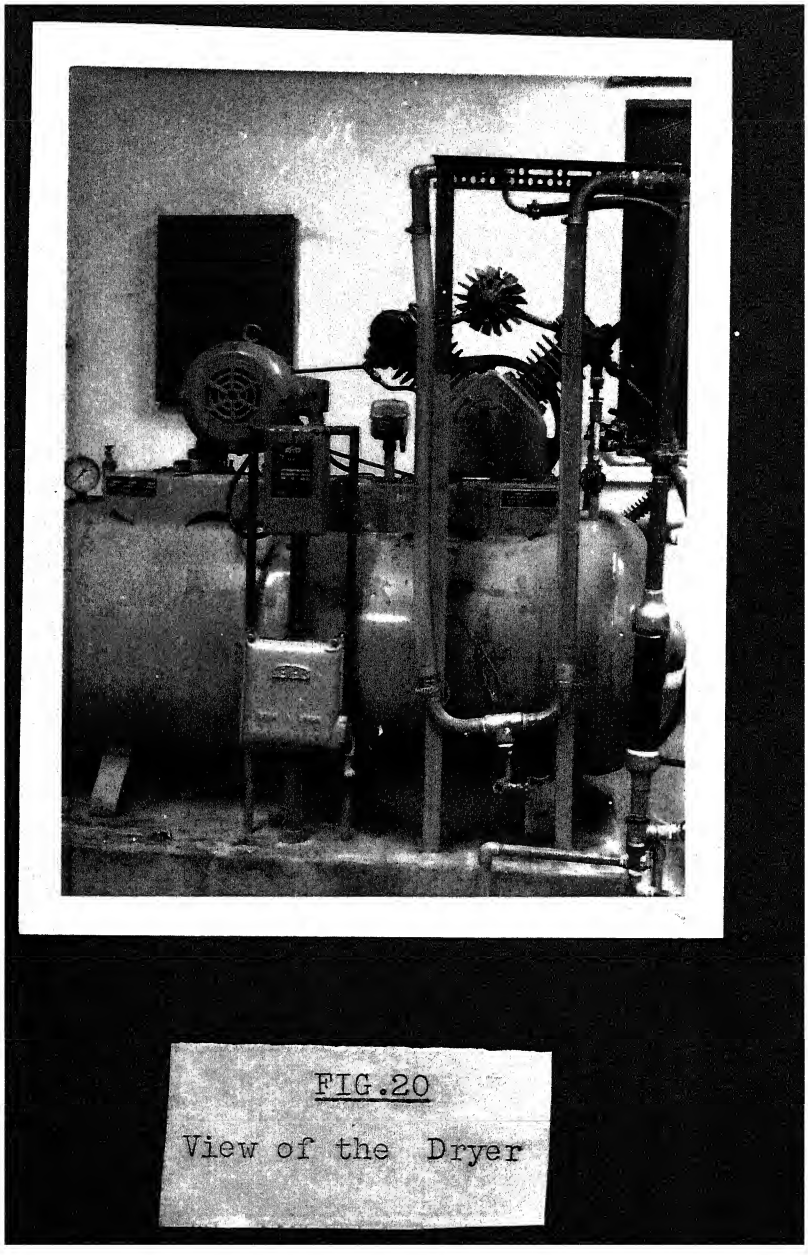

FIG.20

View of the Dryer

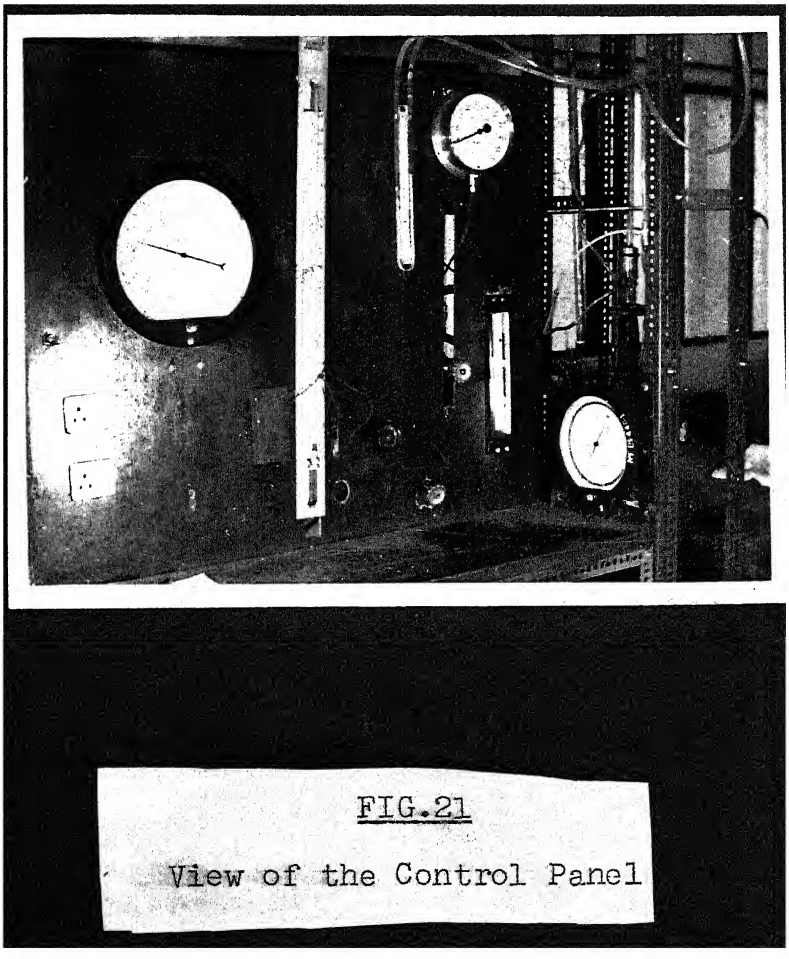

FIG.21

View of the Control Panel

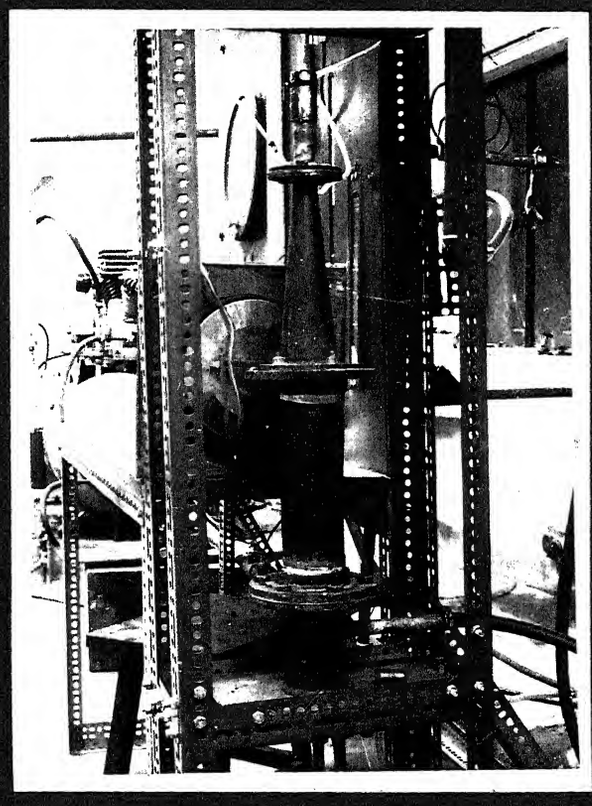

FIG.22

View of the mixing chamber